การประยุกต์ใช้ท่อนาโนคาร์บอนแบบผนังหลายชั้นที่มีเหล็กในตัว เพื่อการกำจัดยาปฏิชีวนะในน้ำ

นางสาวกนกวรรณ โสวิชัย

วิทยานิพนธ์นี้เป็นส่วนหนึ่งของการศึกษาตามหลักสูตรปริญญาวิศวกรรมศาสตรมหาบัณฑิต
สาขาวิชาวิศวกรรมเคมี ภาควิชาวิศวกรรมเคมี
คณะวิศวกรรมศาสตร์ จุฬาลงกรณ์มหาวิทยาลัย
ปีการศึกษา 2555

APPLICATION OF FE-FILLED MULTI-WALLED CARBON NANOTUBES FOR REMOVAL OF ANTIBIOTICS FROM AQUEOUS SOLUTION

Miss Kanokwan Sowichai

A Thesis Submitted in Partial Fulfillment of the Requirements
for the Degree of Master of Engineering Program in Chemical Engineering
Department of Chemical Engineering
Faculty of Engineering
Chulalongkorn University
Academic Year 2012

Thesis Title	APPLICATION OF FE-FILLED MULTI-WALLED CARBON NANOTUBES FOR REMOVAL OF ANTIBIOTICS FROM AQUEOUS SOLUTION
By	Miss Kanokwan Sowichai
Field of Study	Chemical Engineering
Thesis Advisor	Associate Professor Tawatchai Charinpanitkul, D.Eng.
Thesis Co-advisor	Sitthisuntorn Supothina, Ph.D.

Accepted by the Faculty of Engineering, Chulalongkorn University in Partial Fulfillment of the Requirements for the Master's Degree

.....Dean of the Faculty of Engineering
(Associate Professor Boonsom Lerdhirunwong, Dr.Ing.)

THESIS COMMITTEE

.....Chairman
(Associate Professor Sarawut Rimdusit, Ph.D.)

.....Thesis Advisor
(Associate Professor Tawatchai Charinpanitkul, D.Eng.)

.....Thesis Co-advisor
(Sitthisuntorn Supothina, Ph.D.)

.....Examiner
(Assistant Professor Nattaporn Tonanon, D.Eng.)

.....External Examiner
(Assistant Professor Sittinun Tawkaew, D.Eng.)

กนกวรรณ โสวิชัย : การประยุกต์ใช้ท่อนาโนคาร์บอนแบบผนังหลายชั้นที่มีเหล็กในตัวเพื่อการกำจัดยาปฏิชีวนะในน้ำ (APPLICATION OF FE-FILLED MULTI-WALLED CARBON NANOTUBES FOR REMOVAL OF ANTIBIOTICS FROM AQUEOUS SOLUTION) อ. ที่ปรึกษาวิทยานิพนธ์หลัก: รศ.ดร. ธวัชชัย ชรินพาณิชกุล, อ. ที่ปรึกษาวิทยานิพนธ์ร่วม: ดร.สิทธิสุนทร สุโพธิณะ, 89 หน้า.

งานวิจัยนี้ มุ่งเน้นในการประยุกต์ใช้ท่อนาโนคาร์บอนแบบผนังหลายชั้นที่มีเหล็กในตัวเป็นตัวดูดซับยาปฏิชีวนะที่ปนเปื้อนในน้ำ โดยท่อนาโนคาร์บอนแบบผนังหลายชั้นที่มีเหล็กในตัวสามารถสังเคราะห์ได้ด้วยวิธีการไพโรไลซิสร่วมระหว่างกลีเซอรอลและเฟอร์โรซีน จากนั้นทำการบำบัดท่อคาร์บอนระดับนาโนเมตรแบบผนังหลายชั้นที่มีเหล็กในตัวด้วยกรดผสมระหว่างกรดไนตริกและกรดซัลฟิวริก ผลจากการวิเคราะห์พบว่า ท่อนาโนคาร์บอนแบบผนังหลายชั้นที่มีเหล็กในตัวที่ผ่านการบำบัดด้วยกรดแล้วมีหมู่ฟังก์ชันของกรดคาร์บอกซิลิกเกิดขึ้นบนพื้นผิว อีกทั้งยังส่งผลให้มีค่าความเป็นประจุลบบนพื้นผิวเพิ่มมากขึ้น

สำหรับการประยุกต์ใช้ท่อนาโนคาร์บอนแบบผนังหลายชั้นที่มีเหล็กในตัวเป็นตัวดูดซับ เพื่อใช้ในการกำจัดยาปฏิชีวนะที่ปนเปื้อนอยู่ในน้ำ ในงานวิจัยนี้ได้ใช้ยาเตตร้าไซคลินและเอนโรฟอกซาซินเป็นตัวแทนของยาปฏิชีวนะที่ปนเปื้อนในน้ำ ผลจากการศึกษาพบว่า ท่อนาโนคาร์บอนแบบผนังหลายชั้นที่มีเหล็กในตัวที่ยังไม่ผ่านการบำบัดด้วยกรดสามารถดูดซับเตตร้าไซคลินได้สูงกว่าตัวที่ผ่านการบำบัดแล้ว โดยสามารถดูดซับได้ 92% ซึ่งสามารถถดูดซับยาปฏิชีวนะทั้งสองชนิดได้ดีในช่วงความเป็นกรด – ด่างระหว่าง 5 – 7 และเมื่อค่าความเป็นกรด – ด่างต่ำลงหรือเพิ่มสูงขึ้น ประสิทธิภาพการดูดซับจะต่ำลง ทั้งนี้เป็นผลมาจากการแตกตัวของยาปฏิชีวนะในค่าความเป็นกรด – ด่าง ที่แตกต่างกันจะทำให้มีลักษณะประจุที่แตกต่างกัน และประกอบกับความเป็นประจุบนพื้นผิวของท่อนาโนคาร์บอนแบบผนังหลายชั้นที่มีเหล็กในตัวด้วย ผลจากการศึกษาผลกระทบของอุณหภูมิ พบว่า ท่อนาโนคาร์บอนแบบผนังหลายชั้นที่มีเหล็กในตัวสามารถดูดซับยาปฏิชีวนะทั้งสองได้สูงขึ้นเมื่ออุณหภูมิของระบบเพิ่มขึ้น โดยสามารถเข้าสู่สมดุลภายใน 1 และ 3 ชั่วโมงสำหรับการดูดซับเตตร้าไซคลินและเอนโรฟอกซาซินตามลำดับ ซึ่งสมดุลการดูดซับของยาปฏิชีวนะทั้งสองสอดคล้องกับแบบจำลองของแลงเมียร์และมีจลนพลศาสตร์ของการดูดซับสอดคล้องกับแบบจำลองทางคณิตศาสตร์จลนพลศาสตร์การดูดซับอันดับสองเทียม และผลจากการศึกษาทางเทอร์โมไดนามิกส์ พบว่า กระบวนการดูดซับเป็นระบบดูดความร้อนที่สามารถเกิดขึ้นได้เอง

ภาควิชา วิศวกรรมเคมี ลายมือชื่อนิสิต .....

สาขาวิชา วิศวกรรมเคมี ลายมือชื่อ อ.ที่ปรึกษาวิทยานิพนธ์หลัก .....

ปีการศึกษา 2555 ลายมือชื่อ อ.ที่ปรึกษาวิทยานิพนธ์ร่วม .....

5370393821: MAJOR CHEMICAL ENGINEERING
KEYWORDS: MULTI-WALLED CARBON NANOTUBES/ANTIBIOTICS/ ADSORPTION/TETRACYCLINE/ ENROFLOXACIN

KANOKWAN SOWICHAI: APPLICATION OF FE-FILLED MULTI-WALLED CARBON NANOTUBES FOR REMOVAL OF ANTIBIOTICS FROM AQUEOUS SOLUTION.
ADVISOR: ASSOC. PROF. TAWATCHAI CHARINPANITKUL, D.Eng., CO-ADVISOR : SITTHISUNTORN SUPOTHINA, Ph.D., 89 pp.

The aim of this research is to investigate the feasibility of utilizing Fe-filled multi-wall carbon nanotubes synthesized by co-pyrolysis of glycerol and ferrocene as an adsorbent for removal of antibiotics from aqueous solution. Then synthesized Fe-filled MWCNTs were also treated by H_2SO_4/HNO_3. It was found that the carboxylic acid was produced on surface of acid treated Fe-filled MWCNTs, thereby improving negatively charged on their surface.

Synthesized Fe-filled MWCNTs were employed for adsorption of antibiotics included tetracycline and enrofloxacin. From the results, pristine Fe-filled MWCNTs could better adsorb tetracycline than acid treated Fe-filled MWCNTs, about 92%. The adsorption efficiency of both tetracycline and enrofloxacin onto pristine Fe-filled MWCNTs increased when pH was increased from 5 – 7 and then decreased significantly as the pH lower or higher than this range. Both adsorption capacity of tetracycline and enrofloxacin increased with temperature increased. In addition, tetracycline could reach equilibrium within 1 hr while adsorption capacity of enrofloxacin did not change significantly after 3 hr. Langmuir model and the pseudo-second-order kinetic model are well used to describe the adsorption for tetracycline and enrofloxacin onto pristine Fe-filled MWCNTs. The nature of adsorption process is the endothermic and spontaneous that was described by thermodynamic parameters.

Department : Chemical Engineering Student's Signature .....
Field of Study : Chemical Engineering Advisor's Signature .....
Academic Year : 2012 Co-advisor's Signature .....

ACKNOWLEDGEMENTS

I am very thankful to my thesis advisor and co-advisor, Assoc Prof. Tawatchai Charinpanitkul and Dr. Sitthisuntorn Supothina, Department of Chemical Engineering, Chulalongkorn University and National Metal and Materials Technology Center (MTEC), respectively for their advice and encouragement throughout the course of this work. Their unwavering support when my research had a rough time, they kept me sailing to accomplish this research. Moreover, I am also thankful to Assoc. Prof. Sarawut Rimdusit, Assist. Prof. Nattaporn Tonanon and Assist. Prof. Sittinun Tawkaew, for their guidance and participation as my thesis committee.

I would like to acknowledge the Centennial Fund of Chulalongkorn University for the partial financial support to this work. This work was also partially supported by National Metal and Materials Technology Center (MTEC).

I would like to thank Miss On-uma Nimittrakoolchai, National Metal and Materials Technology Center (MTEC), for her kindliness and guidance to use equipments and analyzer at MTEC. She was a source of my inspiration, when I was internship that could pave the way for my thesis.

I would like to thank all members of Center of Excellence in Particle Technology for their help, suggestion and warm collaborations.

Furthermore, I would like to thank Mr. Wanut Jirathitiwong and Miss Jirapan Ponlok for their personal encouragement at all time. They cared me when I conducted hard experiments all night.

Above all, I would like to express my cordial and deep thanks to my family for their love and personal support at all time. They were always with me during the accomplishment of this research.

CONTENTS

Page

Page

Page

Page

LIST OF TABLES

Table **Page**

LIST OF FIGURES

Figure **Page**

Figure **Page**

Figure **Page**

CHAPTER I
INTRODUCTION

1.1 Background and Motivation

Antibiotics have been widely used therapeutically in humans and animals, and as to prevent or treat infections in humans or animals as the spread of diseases or promoting faster growth in aquaculture and livestock operations. Because of their large usage, the antibiotics are spread in the environment via municipal, wastewater outflow from industrial, wastewater sludge and agricultural runoff. They may cause great environmental threats as a result of serious side-effects for their broad-spectrum antimicrobial properties [1]. In addition, they may induce increasing the resistance of bacteria against drugs and threatening the survival of microorganisms, leading to serious environmental damages. Furthermore, they have been reported that free antibiotics could critically disturb the natural bacteria ecosystems, due to a serious threat to human health [2]. Consequently, it is necessary to develop some efficient and cost-effective technologies to remove such compounds.

Adsorption technology with no chemical degradation is a well established science used in industry for treatment of wastewater contaminated with organic compounds due to its simplicity, efficiency and economy [3]. It is well known that adsorption is a separation process which molecules or atoms in fluid phase have to adhere on the solid surface. Currently, activated carbons including zeolites, clays, biomass and polymeric materials are used as adsorbent primarily. However, these adsorbents are also low adsorption capacities and separation inconvenience [4] that would be the main drawback. Therefore, research efforts are still needed to carry out investigation for new promising substance to replace conventional adsorbents.

Carbon nanotubes (CNTs) are among new members in the carbon family with unique properties such as exceptional mechanical, excellent electrical and potential applications that have been attracted to attention by a lot of researchers as long as they were officially reported by Iijima in 1991 [5]. In general, CNTs can be classified into single-walled carbon nanotubes (SWCNTs) and multi-walled carbon nanotubes (MWCNTs) by graphene layers constituting of the wall. They are have excellent

structures such as large specific surface areas, small size, hollow and layered structures that could be designed for relatively new adsorbent application which would be superior to other conventional adsorbents. CNTs have gained increasing attention from adsorption point of view since Long and Yang first reported that CNTs were more efficient for the removal of dioxins when compared with activated carbon [6]. However, there are very limited reports on the antibiotics adsorption of CNTs. By the way, collection of such CNTs from adsorptive process after the saturation would be an emerging issue which would require further investigation. Meanwhile magnetic separation technology has gradually attracted growing attention of many researchers and scientists as a rapid and effective technology for separating magnetic materials. This technology possesses a major advantage over other conventional separation techniques in terms of economy, high capacity, short operation time and no contamination [7]. The combination technology between magnetic separation and adsorption is therefore of a great potential interest and has been widely used for purification applications.

In this work, the co-pyrolysis of ferrocene and glycerol was applied for synthesizing Fe-filled multi-walled carbon nanotubes (Fe-filled MWCNTs), which can be higher effectiveness as adsorbent and also convenience separating than conventional adsorbents. Moreover, it was carefully characterized before investigating their adsorption properties for the removal of antibiotics. The antibiotics studied here included tetracycline and enrofloxacin. The adsorption characteristics and external factors were also verified.

1.2 Objectives of the research

The objective of this research is to investigate feasibility of utilizing Fe-filled multi-walled carbon nanotubes (Fe-filled MWCNTs) synthesizing by co-pyrolysis of ferrocene and glycerol for removal of antibiotics from aqueous solution in batch adsorption system.

1.3 Scope of the research

1.3.1 Synthesis of Fe-filled Multi-walled Carbon nanotubes (Fe-filled MWCNTs)

The Fe-filled MWCNTs were synthesized by co-pyrolysis of ferrocene and glycerol, according to the condition reported by Akrapattangkul [43].

- 1: 5 molar ratios of ferrocene and glycerol
- 900^{o}C of the pyrolysis temperature
- Nitrogen gas as carrier gas

1.3.2 Acid treatments of the synthesized Fe-filled MWCNTs

The Fe-filled MWCNTs were treated by a 1:3 ratios of concentrated H_2SO_4/HNO_3 mixture, according to the procedure reported by Blanchard et al [32].

1.3.3 Characterization methods of the synthesized products

The synthesized products from co-pyrolysis also the synthesized Fe-filled MWCNTs after treatment were characterized by techniques as follow:

- Scanning electron microscope (SEM) and Transmission electron microscope (TEM) were used to observe the morphology
- X-ray diffraction (XRD) was used to characterize the structure and composition
- Fourier transform infrared (FT-IR) spectrometer was used to characterize functional group on their surfaces.
- Zetasizer was used to measure the surface charge properties by making measurements of zeta potential.

1.3.4 The adsorption of antibiotics from aqueous solution by the synthesized Fe-filled MWCNTs

All of these experiments were conducted under batch adsorption experiment, which were performed with UV-visible spectrophotometer. The adsorption characteristics and external factors were studied as follow:

1.3.4.1 Effect of adsorbent loading

- The amount of adsorbent loading
- Type of adsorbent loading

1.3.4.2 Effect of initial pH

1.3.4.3 Effect of temperature

- Adsorption isotherms
- Thermodynamic studies
- Adsorption kinetics

1.4 Procedures of the research

- Execution of related literature survey and review
- Preparation of experimental materials using in this research
- Synthesis of Fe-filled Multi-walled Carbon nanotubes (Fe-filled MWCNTs) by co-pyrolysis
- Characterization of the synthesized Fe-filled MWCNTs properties by SEM, TEM , XRD, FT-IR and Zetasizer
- Preparation of modify the synthesized Fe-filled MWCNTs by H_2SO_4/HNO_3 mixture oxidation
- Characterization of acid-treated Fe-filled MWCNTs properties by SEM, TEM, FT-IR and Zetasizer
- Execution of adsorption characteristics and external factor effects of antibiotics adsorption on Fe-filled MWCNTs
- Conducting discussion and conclusion of experimental results
- Summarization of all experimental results to write thesis

1.5 Expected benefit

Expected benefits to be obtained from this research would be the knowledge in synthesis of Fe-filled MWCNTs by co-pyrolysis of glycerol and ferrocene, which would be applied to removal antibiotics contaminated in water.

CHAPTER II
THEORY AND LITERATURE REVIEW

2.1 Carbon nanotubes (CNTs)

Carbon nanotubes (CNTs) are member of carbon based materials which have been discovered at about 20 years ago by Ijima in 1991 [5]. They have generated developing in most areas of science and engineering technology due to their unique physical and chemical properties. Their unique properties attributed including superlative mechanical, thermal and electronic properties have not displayed in previous material. Based on their unique properties have opened new research areas in physics, chemistry and also materials science.

Carbon nanotubes (CNTs) are allotropes of carbon with a cylindrical structure that built from sp^2 carbon units and consists of honeycomb lattices known as grapheme sheet. Usually, they can be classified according to the number of concentric tubes in single-wall or multi-walls. Single walled nanotubes (SWCNTs) consist of a single sheet of graphene rolled up to form a cylinder with a typical diameter of few nanometers while length up to centimeters. Multi-walled nanotubes (MWCNTs) consist of multiple rolled layers of graphene of such concentric tubes formed with the distance between layers about 0.34 – 0.36 nm and also it have diameters from 2-100 nm and lengths up to millimeters as shown in Figure 2.1 (a) and (b), respectively.

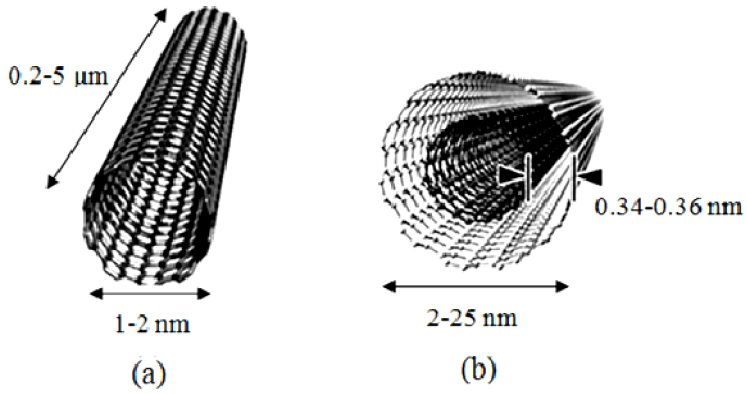

Figure 2. 1 Structures of SWCNTs (a) and MWCNTs (b)
(http://jnm.snmjournals.org/content/48/7/1039/F1.expansion.html)

2.1.1 Synthesis of CNTs

The are several methods to generate CNTs which are difference in how carbon atoms are produced from carbon sources, including sublimation of graphite by arc discharge and laser ablation method and decomposition of carbon-containing molecules by chemical vapor deposition method.

2.1.1.1 Arc discharge method

This method is carried out at a high temperature, using a high electric current. Two graphite rods, one acting as an anode and the other as a cathode, are placed close together in an inert atmosphere of helium gas or argon. An electric current is passed between the two rods, forming a hot, bright arc of electricity that vaporizes carbon from the anode and generates plasma of carbon and helium. The carbon from the plasma re-condenses on the cathode to form mostly multiwalled nanotubes (MWCNT). Two kind of synthesis can be performed with the arc: evaporation of pure graphite and co-vaporization of graphite and metal. The arc discharge method for generating MWCNTs appears very simple, but it is difficult to obtain high yields and requires careful to control of experimental conditions.

2.1.1.2 Laser ablation method

This method can generate CNTs with the highest quality and high purity of SWCNTs [8]. In this method, a rod of graphite as carbon source and catalytic metal (Co, Nb, Pt, Ni, Cu or a binary combination thereof) mixture is ablated at its surface by laser in an inert atmosphere, forming a carbon vapor from a graphite rod. The carbon vapor re-condenses to form predominantly SWCNTs when are carried to a water-cooled by inert carrier gas (helium or argon). The parameters which effect on tube diameter of CNTs are the furnace temperature and the catalyst used.

2.1.1.3 Chemical Vapor Deposition

This method is achieved by taking a carbon source in the gas phase and using an energy source, such as plasma (plasma enhancement CVD) or resistively heated coil (thermal CVD), to give energy to a gaseous carbon molecule. The energy source is used to decompose the molecule into a reactive radical species. The reactive species

diffuse into the catalyst nanoparticles that the catalyst acts like “seed” and the nanotube grows out from it, growing longer and longer as more carbon atoms are released from the gas. The working conditions such as type of carbon and catalyst source affect the characteristics of the produced CNTs by CVD. This method can produce both SWCNTs and MWCNT, depending on the temperature and other growth parameters. Moreover, the large quantities of nanotubes can be generated by this method. Therefore, this method is the first candidate for industrial applications.

2.2 Antibiotics

Antibiotics are compound or chemical substance derivable from a microorganism produced by chemical synthesis with pharmaceutical activity, which are used as active principle in several drugs [9]. They have the ability to kill or to inhibit the growth of other microorganism and cure infections. Antibiotics target microorganisms such as bacteria, fungi and parasites. If antibiotics are overused or used incorrectly there is a chance that the bacteria will become resistant - the antibiotic becomes less effective against that type of bacterium.

Antibiotics are commonly classified according to their chemical structure as:

- Beta-lactams: penicillins, cephalosporins (1^{st} generation, 2^{nd} generation and 3^{rd} generation) monobactams and carbapenems
- Aminoglycosides
- Tetracyclines
- Macrolides
- Sulfonamides
- Quinolones
- Azoles

In addition, antibiotics can be grouped based on mechanism of action or spectrum of activity which target bacterial functions or growth processes. The three main mechanisms of action for antibiotics are [10]:

- Inhibition of the bacterial cell wall synthesis are Beta-lactums
- Inhibition of protein synthesis are aminoglycocides, tetracyclines and macrolides

- Inhibition of interfere with essential bacterial enzymes synthesis are sulfonamides, quinolones and azoles.

Due to the widespread use (from human or veterinary application) and not well inform to control and to use of antibiotics, bacteria are consistently exposed to these drugs. Although many bacteria die with antibiotics, this continuous exposure causes the development of bacterial resistance to the drugs' effects. This is a main concern since, if bacteria become resistant and no responding to particular antibiotics, the treatment of humans will be compromised. In order to control resistance there must be reinforcement on the suitable use of antibiotics, which would maximize the clinical therapeutic effect, and minimize both drug-related toxicity and resistance itself [11].

2.2.1 Tetracyclines

Tetracyclines (TCs) are broad-spectrum antibiotics that perform as such at ribosomal level where they interfere with protein synthesis. They were discovered in 1948 as natural fermentation products of a soil bacterium *Streptomyces aureofaciens*. The first chemically purified tetracycline in six year later was chlortetracycline [12]. At present, three groups of tetracyclines are available including tetracycline natural products, tetracycline semi-synthetic compound (SST) and chemically modified tetracycline (CMT) [13].

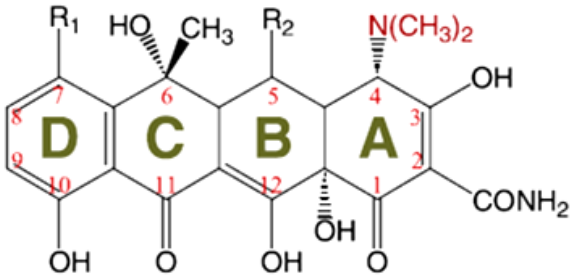

Figure 2.2 Structure of tetracyclines (TCs) [14]

All tetracycline chemical structures consist of a tetracyclic naphtacene carboxamide ring structure with surrounding upper and lower peripheral zones as shown in Figure 2.2. Tetracyclines with antibiotic activity have a dimethylamine

group at carbon 4 (C4) in ring A while removing of the dimethylamino group from C4 enhances non-antibiotic action [12, 13]

Table 2.1 Chemical structures and relevant data for tetracyclines (TCs) [14, 15]

Compounds	Formula	R_1	R_2	pK_{a1}	pK_{a2}	pK_{a3}
Tetracycline (TTC)	$C_{22}H_{24}N_2O_8$	H	H	3.3	7.7	9.7
Oxytetracycline (OTC)	$C_{22}H_{24}N_2O_9$	H	OH	3.3	7.3	9.1
Chlortetracycline (CTC)	$C_{22}H_{23}ClN_2O_8$	Cl	H	3.3	7.5	9.3

2.2.2 Quinolones

Quinolones are commonly classified as synthetic antibiotics and were discovered in the 1960s while anti-malaria pharmaceuticals were being developed. The basic structure common to all quinolones are shown in Figure 2.3. Nalidixic acid was the first quinolone discovered in 1962, arranging the first generation of quinolones. Since then, four generations of quinolones have been developed, and more compounds are being studied. Subject to the diversity of their various ring structures, the quinolones have common functional groups that are essential for their antimicrobial activity, these are positions 2, 3 and 4 [16]. In spite of positions, modifications in other positions have been generated, leading to different physical, chemical, pharmacokinetic, and antimicrobial properties in compounds.

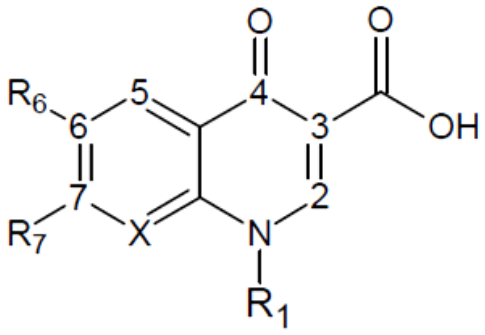

Figure 2.3 Basic structure of a quinolone

For instance, fluoroquinolones (FQs) which is distinguished by a fluorine atom at the position 6 that enhances the activity against both gram-naegative and gram-positive bacteria, as well as mycoplasma and chlamydiae [10]. Figure 2.4 represents some examples of FQs.

FQs have an acidic carboxylic group, with reported pK_a values in the 5.5 to 6.6 range, and an amino group with pKa values for the protonated amino form in the 7.2 to 8.9 range.

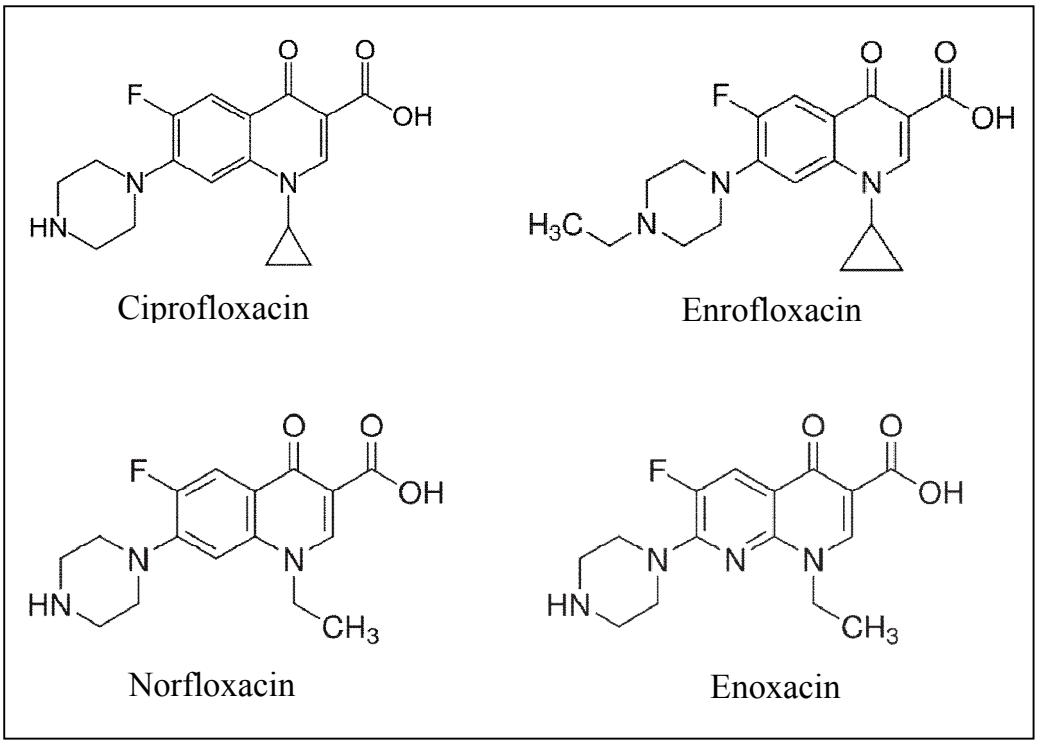

Figure 2.4 Examples of fluoroquinolones

2.3 Adsorption process

Adsorption is a surface phenomenon of separation process based on equilibrium and material balance. When a solution containing absorbable solute comes into contact with a solid with a highly porous surface structure, liquid–solid intermolecular forces of attraction cause some of the solute molecules from the solution to be concentrated or deposited at the solid surface. The solute retained (on the solid surface) in adsorption processes is called adsorbate, whereas the solid on which it is retained is called as an adsorbent. This surface accumulation of adsorbate on adsorbent is called adsorption. This creation of an adsorbed phase having a

composition different from that of the bulk fluid phase forms the basis of separation by adsorption technology. As the adsorption progress, an equilibrium of adsorption of the solute between the solution and adsorbent is attained (where the adsorption of solute is from the bulk onto the adsorbent is minimum).

2.3.1 Type of adsorption

Based on surface chemistry and forces involved in adsorption, there are three interfaces involved in adsorption including adsorbate-adsorbent, adsorbate-water and water-adsorbent. The forces active at each of these interfaces are listed in Table 2.2. Some of the forces that occur between the adsorbent surface and adsorbates are depicted in Figure 2.5

Table 2.2 Summary of forces that are active at three interfaces involved in adsorption [17].

Force	**Approximate Energy of Interaction (kJ/mol)**	**Interface**		
		Adsorbate/ Adsorbent	Adsorbates/ Water	Water/ Adsorbent
Electrostatic attraction	> 42	Yes	No	No
Electrostatic repulsion	> 42	Yes	No	No
Ionic species-neutral species attraction		Yes	No	No
Covalent bonding	> 42	Yes	No	No
Ionic species-dipole Attraction	< 8	Yes	Yes	Yes
Dipole-dipole attraction	< 8	Yes	Yes	Yes
Dipole-induced dipole Attraction	< 8	Yes	Yes	Yes
Hydrogen bonding	8 – 42	Yes	Yes	Yes
van der Waals attraction	8 – 42	Yes	Yes	Yes

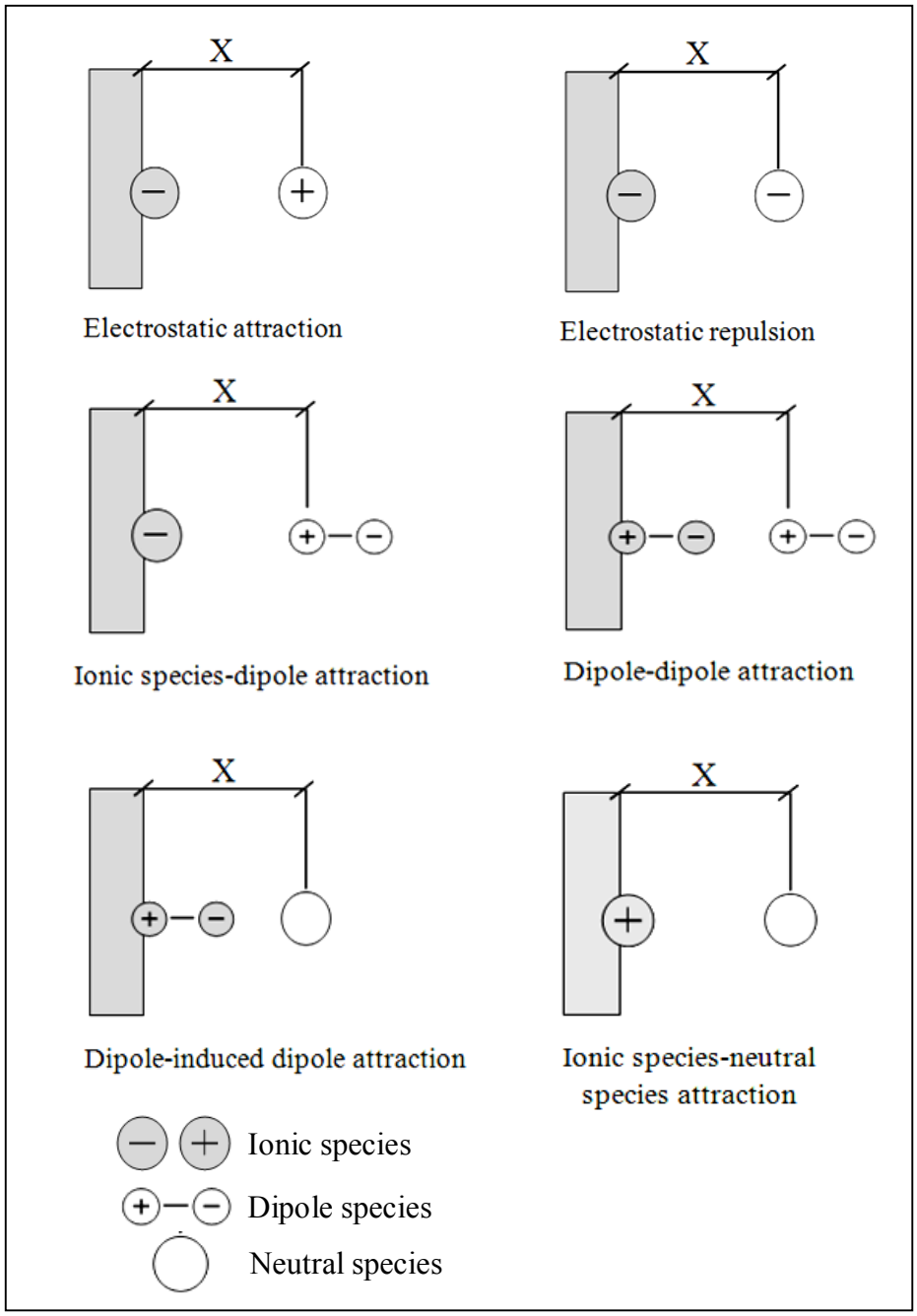

Figure 2.5 Surface functional groups and forces of attraction [17]

2.3.1.1 Chemical adsorption or Chemisorption

Chemical adsorption, occurs when the adsorbate reacts with the surface to form a covalent bond or an ionic bond. The attraction between adsorbent and adsorbate approximates that of a covalent or electrostatic chemical bond between

atoms, with shorter bond length and higher bond energy. The accumulation of adsorbates bound on an adsorbent surface cannot accumulate more than one molecular layer, due to the specificity of the bond between adsorbate and surface. The bond may also be specific to particular sites or functional groups on the surface of the adsorbent. The charged surface groups attract the opposite charges and expel like charges as follows to Coulomb's law [17]. In general, chemical adsorption is seldom reversible, and a wide range of enthalpy changes may occur, though the typical energies are 15-100 kcal/mole.

2.3.1.2 Physical adsorption or Physisorption

Adsorbates are said to operate physical adsorption if the forces of attraction involve only physical forces that except covalent bonding with the surface and electrostatic attraction of unlike charges. Physical adsorption is less specific for which compounds adsorb to surface sites, has weaker forces and energies of bonding**.** It is often interested to water treatment, adsorbing of organic adsorbates from water (polar solvent) onto a nonpolar adsorbent such as activated carbon. Generally, attraction between an adsorbate and polar solvent is weaker for adsorbates that are less polar or have lower solubility. The attraction between an adsorbate and nonpolar adsorbent surface increase with increasing polarizability and size, which are mainly related to van der Waals forces. This form of adsorption is also known as hydrophobic bonding that hydrophobic compounds will adsorb on carbon more strongly [17]. In addition, physical adsorption has a comparatively low enthalpy of adsorption, typically is only 2-20 kcal/mole and is generally more reversible.

2.3.2 Adsorption isotherms

Adsorption isotherms can use to quantify the affinity of the adsorbate for an adsorbent, which are used to explain the amount of adsorbate that can be adsorbed onto an adsorbent at equilibrium and at a constant temperature. They are carried out by exposing known quantity of adsorbate in a constant volume of liquid, preventing the loss of adsorbate in situations. At the reached equilibrium, the aqueous-phase concentration of the adsorbate is measured and the amount of absorbate adsorbed onto adsorbent at equilibrium (mg/g) is calculated following:

$$Q_e = (\frac{C_0 - C_e}{M}) \times V, \quad (2.1)$$

where Q_e is the amount of adsorbate adsorbed on adsorbent at equilibrium (mg/g), C_0 is the initial concentration of adsorbate (mg/L), C_e is the equilibrium concentration of adsorbate (mg/L), V is the volume of solution (L) and M is the mass of the adsorbent (g).

In general, if adsorption is reversible, the adsorption and desorption rates equal each other for the system to be steady state. The steady state is assumed that is a well-mixed condition by the concentration profile, is also an equilibrium state because there are no net molecular fluxes. Therefore, Q_e and C_e are the amount of adsorbate adsorbed onto adsorbent (mg/g) and the adsorbate concentration (mg/L) at equilibrium [18].

Equations developed by Langmuir and Freundlich are often used to described the amount of equilibrium adsorbate adsorbed onto adsorbent. Details of these isotherm models are presented as follows:

2.3.2.1 Langmuir isotherm

The Langmuir adsorption isotherm is used to explain the equilibrium between sureface and solution a reversible chemical equilibrium between species [17]. This isotherm is based on four hypotheses:

- The surface of the adsorbent is uniform, which all the adsorption sites are equal.
- Adsorbed molecules do not interact.
- All adsorption occurs through the same mechanism.
- At the maximum adsorption, only a monolayer is adsorbed

The theoretical Langmuir isotherm is acceptable for adsorption of a solute from a liquid solution as monolayer adsorption on a surface containing a finite number of agreement sites. Langmuir isotherm model assumes uniform energies of adsorption onto the surface without transmigration of adsorbate in the plane of the

surface. The Langmuir equation is the most widely used parameter equation following Eq. (2.2)

$$\frac{C_e}{Q_e} = \frac{C_e}{Q_m} + \frac{1}{K_L Q_m}, \tag{2.2}$$

where C_e is the concentration of adsorbate at equilibrium (mg/L), Q_e is the amount of adsorbate adsorbed at equilibrium (mg/g), Q_m is the maximum adsorption capacity (mg/g) and K_L is the Langmuir adsorption equilibrium constant (L/mg). A plot of C_e/Q_e against C_e using Eq. (2.2) results in a straight line with slope and intercept can be determined to Q_m and K_L, respectively.

Furthermore, the shape of the isotherm has been examined with the aim to predict whether an adsorption system is favorable or unfavorable [19]. The essential feature of the Langmuir isotherm can be indicated by mean of "R_L", a dimensionless constant related to as the separation factor or equilibrium parameter. R_L can be calculated using as follow:

$$R_L = \frac{1}{1 + K_L C_0}, \tag{2.3}$$

where C_0 is the initial concentration of adsorbate (mg/L) and K_L is the Langmuir adsorption equilibrium constant (L/mg). The meanings of R_L calculated are as follow:

$R_L = 0$: The adsorption process is irreversible

$R_L = 1$: Linear adsorption

$R_L > 1$: Unfavorable adsorption

$0 < R_L < 1$: Favorable adsorption

2.3.2.2 Freundlich isotherm

The Freundlich isotherm model assumes that the adsorbent is heterogeneous surface energies and the amount of adsorbed is far below its saturation value, in which the energy term in the Langmuir equation varies as a function of the surface coverage.

This isotherm is the most important multisite adsorption isotherm for rough surface. It is an empirical equation, using to describe for heterogeneous adsorbent as given by:

$$Q_e = K_F C_e^{1/n}, \tag{2.4}$$

Eq. (2.4) can be converted into Eq. (2.5) by using the logarithmic form:

$$\log Q_e = \log K_F + \frac{1}{n} \log C_e, \tag{2.5}$$

where Q_e is the amount of adsorbated adsorbed at equilibrium (mg/g), C_e is the concentration of adsorbate at equilibrium (mg/L), K_F is the Freundlich adsorption capacity parameter (mg/g)*(L/mg)^n and n is the Freundlich adsorption intensity parameter (unitless) that range between 0 and 1 [20].

The magnitude of n quantifies the favorability of adsorption and the degree of heterogeneity of the adsorbent surface. For $n = 1$, indicating the adsorption is constant (independent of the solute solution), but for $n < 1$, the adsorption strength decrease with increasing solute concentration [20].

2.4 Literature reviews

2.4.1 Synthesis of Fe-filled multi-walled carbon nanotubes (Fe-filled MWCNTs

Hampel et al. (2006) synthesized of Fe-filled multi-walled carbon nanotubes by chemical vapor deposition (CVD) of ferrocence and cyclopentane. The reaction parameters such as reaction temperature in range of 850 – 950^{o}C, deposition time and precursor concentration were studied as affect to diameter, length and Fe-filling yield of the carbon nanotubes (CNTs). As the results, at 900^{o}C could give well-aligned multi-walled carbon nonotubes (MWCNTs) and also the highest purity have nanotubes grown. The diameter and length of nanotubes are only controlled by the ferrocene concentration in the gas phase. For all temperatures the multi-walled carbon nanotubes were filled of iron yield achieving about 45 wt%. They found for the

sample synthesized high are ferromagnetic of ferrite and austenite, showing coercivity are higher than in bulk iron [21].

Zhao et al. (2006) studied the influences factors on the growth morphology of carbon nanotubes, such as reaction time and different carrier gases concerning hydrogen and nitrogen as well as no carrier gas to synthesis of carbon nanotubes (CNTs) using chemical vapor deposition (CVD) of methane on catalyst of Ni-Cu-Al powder. The reaction time brought no significant influence to the diameter of CNTs, but prolonging the reaction time could increase the average length of the CNTs. The highest of production rate and yield of synthesized carbon nanotubes for the nitrogen as carrier gas could be used that relatively pure compared with CNTs hydrogen carrier gas and also no carrier gas. The nitrogen carrier gas has not reacted in the methane decomposition, which was assumed to keep the catalyst surface clean so that carbon atom supply rate was higher than that with hydrogen carrier gas [22].

Liu et al. (2008) reported that the different formation of magnetic nanostructures such as Fe nanoparticles (Fe-NPs) adhering to singlewalled carbon nanotubes, carbon-encapsulated Fe-NPs, Fe-NP decorated multi-walled carbon nanotubes (MWCNTs), and Fe-filled MWCNTs were synthesized by the pyrolysis of pure ferrocene under the argon atmosphere. These formations can be controlled by the size of Fe particles as catalyst, which depend on the sublimation temperature of ferrocene. When ferrocene was sublimated at less than 110^{o}C, 110 - 140^{o}C, 140 – 160^{o}C and 160 – 400^{o}C, can produce Fe-NPs adhering to SWCNTs, CNPs, Fe-NP decorated MWCNTs, and Fe-filled MWCNTs, respectively [23].

Musso et al. (2008) synthesized carbon nanotubes (CNTs) using chemical vapor deposition (CVD) of camphor and ferrocene with a mass ratio of 20:1. A mixture of camphor and ferrocene was prepared in a flask with heating up to 220^{o}C which connected to the quartz tube reactor. The nitrogen was used carrying vaporized mixture into the reactor where inserted the silicon substrate. The effect of temperature on the formation of the CNTs on crystalline silicon substrate was investigated with heating up in a range of 800 – 1000^{o}C. At a substrate temperature in the ranges of 650-900 ºC, a carpet of vertically CNTs was generated on silicon substrate. On the

other hand, the silicon substrate in the temperature ranges of 950-1070 ºC generated the formation of a nanographite layer and carbon fibers [24].

Cheng et al. (2009) synthesized Fe-filled carbon nanotubes using chemical vapor deposition (CVD) of ethanol as the carbon source and ferrocene as a catalyst precursor for CNTs growth and source of iron and also mixed gases of high purity nitrogen and 3% of hydrogen per argon as carrier gas were used. The synthesized Fe-filled CNTs could be formed at 800^{o}C for 30 minutes reaction time about 10 micrometer in length, with an outer diameter of 20 – 100 nm and inner diameter of 10 – 30 nm. The iron is relatively better filling into CNTs likely iron nanowires. The types of iron filled in CNTs are ferrite α-Fe, austenite γ-Fe and iron carbide Fe_3C that could exhibit magnetic property about average coercivity of 257.05 Gauss [25].

Charinpanitkul et al. (2009) investigated that the co-pyrolysis of naphthalene and ferrocene with a constant ratio of 1:1 loading in a graphite boat could be synthesized the carbon nanoparticles, such as carbon nanotubes (CNTs) and carbon nanocapsules (CNCs) which Fe-filled in their shells. The effect of reaction temperatures were studied in a range of 800 – 1050ºC. The enhance formation of CNCs with lower amount of the CNTs were produced on increasing of temperature. The morphology and size of the carbon nanoparticles also enhanced total yield of products could be depended on the increased reaction temperature [26].

2.4.2 Application of CNTs for removal antibiotics

Wang et al. (2010) investigated different CNTs which were graphitized multiwall CNTs (G-MWCNTs), carboxylated multiwall CNTs (C-MWCNTs) and hydroxylated multiwall CNTs (H-MWCNTs) as adsorbents to adsorb norfloxacin (NOR). The used CNTs were synthesized by the chemical vapor deposition method. G-MWCNTs were produced by treating synthesized CNTs under inert gas at 2800^{o}C for about 240 h. C-MWCNTs and H-MWCNTs were produced by KMnO4 oxidation in HCl solution at different temperatures and different KMnO4 concentrations. The adsorption capacity and isotherm at various temperatures in a rage of 15 – 37^{o}C were obtained by batch experiment. All adsorption isotherms could be well fitted by Freundlich and Polanyi-Manes models. The adsorption capacity revealed that H-MWCNTs adsorbed NOR much higher than G-MWCNTs while C-MWCNTs had

lower adsorption than G-MWCNTs. These results suggested that the surface chemistry was an important factor influencing the adsorption efficiency and also examined the possible mechanisms in NOR-CNTs adsorption which were electrostatic interaction between charged of NOR and CNTs and hydrophobic interaction of the $\pi - \pi$ electron donor – acceptor [27].

Carabineio et al. (2011) studied on the different carbon materials which were activated carbon (AC), carbon nanotubes (CNTs) and carbon xerogel (CX) to adsorb ciprofloxacin (CPX) with also different modification surface. The effect of their surface chemistry on the adsorption of this antibiotic was determined, which were kinetics and isotherms of adsorption. All of carbon materials were treated surface by chemical oxidation method with nitric acid and also thermal treatments, leading to modification their surface chemistry. The optimal of initial concentration of CPX and carbon samples to reach equilibrium time were conducted. The results suggested that AC and CX were treated by thermal treatments to higher adsorption than acid treatment due to the active sites also surface area were more provided, whereas CNTs behave differently, was treated by nitric acid treatment causing to increase the adsorption capacity due to the surface groups on the defect also more opening some of the CNTs endcaps were increased. The kinetic and isotherm of adsorption could be well fitted of the pseudo-second-order and the Langmuir models, respectively [28].

Zhang et al. (2011) used multi-walled carbon nanotubes (MWCNTs) that were functionalized carbon nanotubes (such as hydroxylized, carboxylized and graphitized of CNTs) as adsorbent for batch adsorption sulfamethoxazole (SMX). They studied determining the various mechanisms of antibiotic adsorption on CNTs by cations and to examine the effect of an anion on antibiotic adsorption. Mechanisms of SMX adsorption on CNTs were played roles by electrostatic interaction and hydrophobic interaction, which were affected by cations and anions. On the other hand, the efficiency increasing or decreasing SMX adsorption could be depended on pH [29].

2.4.3 Adsorption of tetracycline (TTC) and enrofloxacin (ENR) with other kinds of adsorbents.

Chen et al. (2011) investigated polyvinylpyrrolidone (PVP-K30) modified nanoscale zero valent iron (NZVI) to remove TTC from aqueous solution over a wide range of conditions, including pH (3 – 10), temperature (25 – 45^{o}C), reactant concentration (50 – 300 mg/L), type of competitive anion and reaction time. From the study results, the efficiency of TTC adsorption by PVP-NZVI depends on pH and temperature that is more effective adsorption in acidic and neutral pH and also high temperature [30].

Gao et al. (2012) used graphene oxide (GO) to treat three representative tetracycline antibiotics, including tetracycline (TTC), oxytetracycline (OTC) and doxycycline (DOX). The effect of pH and salt concentration were studied. From this studied, tetracycline could be adsorbed on graphene oxide via $\pi - \pi$ interaction and cation-π bonding mechanism, due to pH effect. Both oxytetracycline and doxycycline are well fitted with Freundlich isotherm while tetracycline is well fitted by Langmuir isotherm [15].

Ötker et al. (2005) investigated the adsorption capacity of enrofloxacin (ENR) by using natural zeolite. The external factors including pH and temperature were studied. From the results, natural zeolite could well adsorb ENR at low pH and also increase adsorb as temperature increased. Adsorption isotherm could be better fitted with Langmuir model than Freundlich model [31].

Zhang et al. (2011) used multi-walled carbon nanotubes (MWCNTs) for adsorption of tetracycline (TTC) from aqueous solution. The effect of pH, the amount of adsorbent, sorption time and temperature of adsorption process were studied. MWCNTs could more effectively removal of TC about 99.8% also could adsorb in wide range of pH 4.5 – 7. Kinetic adsorption could be fitted in the pseudo-second-order. Adsorption isotherm could be well fitted in the Langmuir model. The adsorption mechanism of TTC onto MWCNT is probably the non-electrostatic $\pi - \pi$ dispersion interaction and hydrophobic interaction [19].

Based on literature reviews, there are some previous works related to the synthesis of carbon nanotubes (CNTs) by thermal co-pyrolysis and also applied as

adsorbent for removal of some antibiotics in aqueous solution that could induce to synthesize Fe-filled MWCNTs in this research by co-pyrolysis with glycerol and ferrocene. Also, the synthesized Fe-filled MWCNTs would apply as promising novel adsorbent for removal antibiotics in aqueous solution. Especially, it could be easily separated from aqueous solution by magnet.

CHAPTER III
EXPERIMENTAL

The experimental is divided into four parts: synthesis of Fe-filled multi-walled carbon nanotubes (Fe-filled MWCNTs), acid treatment of the synthesized Fe-filled MWCNTs by co-pyrolysis, synthesis of magnetic multi-walled carbon nanotubes (M-MWCNTs) by co-precipitation and adsorption of antibiotics by these synthesized adsorbents.

3.1 Synthesis of Fe-filled multi-walled carbon nanotubes (Fe-filled MWCNTs) by co-pyrolysis method

In this work, the co-pyrolysis of glycerol and ferrocene in a single tube furnace reactor was investigated for synthesis the Fe-filled multi-walled carbon nanotubes. This synthesis condition was adopted from Charinpanitkul's research [26]. The experimental setup is shown in Figure 3.1. It consists of an electrical furnace, a quartz tube reactor with inner diameter of 4.1 cm and length of 60 cm, an alumina boat of precursor, silicone stoppers and a dust collector.

Prior to conducting the synthesis, the temperature profile in a quartz tube reactor was measured by an automatic temperature controller. Glycerol (Ajax Chemicals, Boiling point is 290^{o}C) and ferrocene (Sigma-Aldrich, Boiling point is 249^{o}C) are used for precursor as sources of carbon and iron catalyst, respectively. The precursor mixture was mixed at 5:1 molar ratio of glycerol to ferrocene and was loaded into an alumina boat. The alumina boat of a mixture was inserted inside the quartz tube reactor where the temperature was high enough for vaporization of the precursor mixture (following the temperature profile). Nitrogen (99.99% purity, TIG) was flowed inside the quartz tube reactor with a constant flow rate of 100 ml/min for 20 min before heating the furnace up. Then, the furnace was heated up to a designated set point of 900^{o}C under controlling 100 ml/min of nitrogen flow rate. The precursor mixture was decomposed, leading to the atoms of carbon and iron which were then carried by nitrogen through the tube reactor into the hot zone (900^{o}C). The process was conducted for 45 min. Then, the quartz tube reactor was naturally cooled down to room temperature. After that, the synthesized black products accumulated on an inner

wall of the quartz tube were collected for characterizing their morphology and element and for antibiotics adsorption study.

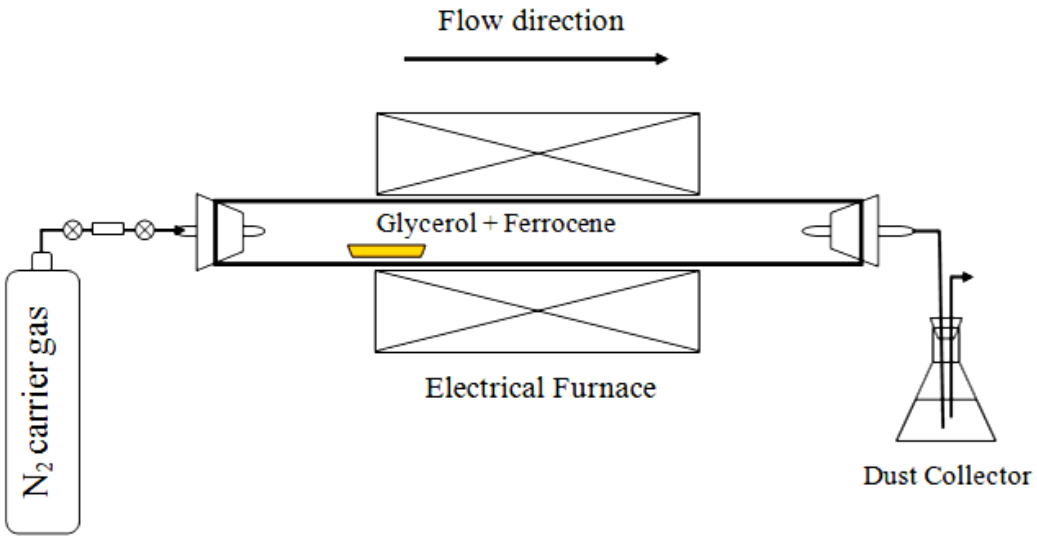

Figure 3.1 Experimental set up for synthesis Fe-filled multi-walled carbon nanotubes by co-pyrolysis of glycerol and ferrocene.

3.2 Acid treatment of synthesized Fe-filled MWCNTs

The synthesized Fe-filled MWCNTs were treated by acid to remove impurities and also to produce the functional group on their surface, according to the procedure reported in the literature [32]. The amount of the synthesized Fe-filled MWCNTs (about 1 g) were dispersed in 200 mL a solution concentrated nitric acid (HNO_3 65% w/w, QRec New Zealand) and sulfuric acid (H_2SO_4 95 – 97% w/w, QRec New Zealand) mixing at volume ratio of 1: 3. The mixture was sonicated at 60^oC for 3 h. After that, it was filtered and washed by de-ionized water and ethanol for several times until the natural pH was reached and subsequently, was dried at 110^oC for overnight.

3.3 Synthesis of magnetic multi-walled carbon nanotubes (M-MWCNTs) by co-precipitation method

Furthermore, in this work also prepared other magnetic adsorbent by co-precipitation method. Magnetic multi-walled carbon nanotubes (M-MWCNTs) were prepared by in situ chemical co-precipitation of Fe^{2+} and Fe^{3+} in the presence of MWCNTs in an alkaline solution.

Commercial MWCNTs bought from Bayer Materials Science were employed to prepare this adsorbent. Prior to depositing iron nanoparticles on commercial MWCNTs, it was also treated by acid according to the procedure reported by Blanchard et al. [32] as same as treatment of Fe-filled MWCNTs. In order to prepare magnetic multi-walled carbon nanotubes (M-MWCNTs), 0.25 g of the acid-treated MWCNTs were dispersed in 100 ml of mixed aqueous solution containing a 1:2 molar ratio of ammonium ferrous sulfate hexahydrate ($(NH_4)_2Fe(SO_4)_2 \cdot 6H_2O$, Changsha, China) and ammonium ferric sulfate dodecahydrate ($NH_4Fe(SO_4)_2 \cdot 12H_2O$, Changsha, China). Ammonium hydroxide solution about 2.5 ml of 8 M was then added dropwise into the suspension which was kept under constant temperature of 50^oC within 30 min under nitrogen atmosphere and ultrasonication in prior to cooling naturally to the room temperature. Finally, the prepared particulate product was separated out from the suspension using a permanent cobalt magnet before being dried under vacuum condition. Then, the prepared M-MWCNTs were characterized before investigating to adsorption.

3.4 Experimental set up for adsorption of antibiotics with synthesized Fe-filled MWCNTs

This study is focused on the adsorption to Fe-filled MWCNTs of tetracycline (TTC) and enrofloxcacin (ENR). The structures of all antibiotics in this study are shown in Figure 3.2

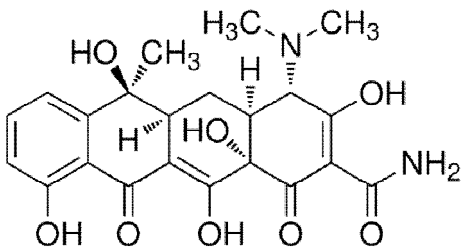

Tetracycline (TTC)

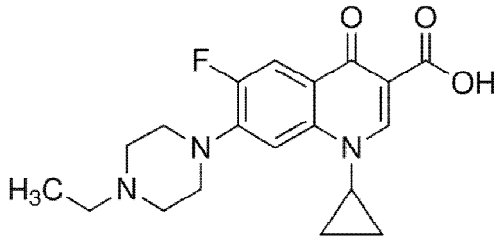

Enrofloxacin (ENR)

Antibiotic compounds	Formula	MW (g/mol)
Tetracycline (TTC)	$C_{22}H_{24}N_2O_8$	444.44
Enrofloxacin (ENR)	$C_{19}H_{22}FN_3O_3$	359.40

Figure 3.2 Structures and relevant data for tetracycline and enrofloxacin (http://www.sigmaaldrich.com)

3.4.1 Preparation of antibiotic solutions

The standard stock solution of tetracycline (TTC, ≥98% purity, Sigma Aldrich Co.) and enrofloxacin (ENR, ≥98% purity, Sigma Aldrich Co) at 100 mg/L were prepared by dissolving in de-ionized water. It was diluted successively to the required concentration.

For preparation of standard curve, the standard stock solutions were diluted at different concentrations. UV-vis spectrophotometer (Shimadzu, Pharma Spec UV-1700) was performed to measure the wavelength of maximum absorbance (λ_{max}) of samples, scanning in the visible range of 200 to 500 nm. Then, the measured data were plotted with the absorbance versus concentration (mg/L) as shown in an Appendix B.

3.4.2 Batch equilibrium adsorption experiments

Batch system was used in adsorption experiment with a magnetic stirrer, which was connected with temperature controller (Electronic contact thermometer, IKA: model ETS-D5) as shown in an Appendix C. All batch experiments were sealed with aluminium foil to prevent light and then were constantly stirred for 24 hr. After

reaching equilibrium, adsorbent was then separated sequentially by magnet and syringe filter prior to spectrophotometer measurement.

- *Studies of effect of adsorbent loading*

For study of the amount of adsorbent loading, the experiments were performed with pristine Fe-filled MWCNTs in range from 4 – 12 mg that were dispersed in the neutral pH with 30 mg/L of antibiotic solutions in a sealed 25 mL flasks. And for study of types of adsorbents loading, pristine Fe-filled MWCNTs and acid treated Fe-filled MWCNTs were studied of the maximum adsorption efficiency of tetracycline. The optimum amount of adsorbents was dispersed in a sealed 25 mL of tetracycline solutions with the neutral pH. The temperature was controlled at 25^{o}C ± 0.5.

- *Studies of effect of initial pH*

To determine the adsorption efficiency at varying pH (3 – 10), the initial pH value of 30 mg/L antibiotic solutions in a sealed 25 mL were adjusted by 0.01M NaOH and HCl. The optimum amount of effective adsorbent was added in solution that controlled temperature at 25^{o}C ± 0.5.

- *Studies of adsorption isotherms*

In order to define the adsorption isotherms at different temperature, batch adsorption experiments were conducted with a sealed 25 mL of antibiotic solution, which tetracycline solutions were 10 – 100 mg/L and enrofloxacin were 10 – 70 mg/L. The optimum amount of effective adsorbent was dispersed in a controlled temperature (25, 40 and 55^{o}C).

3.4.3 Batch kinetic experiments

In order to ascertain the influence of temperature on the adsorption rate of antibiotics, kinetic experiments were carried out. In sealed 500 mL containing 30 mg/L of antibiotic solutions and the optimum amount of effective adsorbent were stirred in a controlled temperature (25, 40 and 55^{o}C) and 3 mL of samples were taken periodically. Every samples were separated sequentially by magnet and syringe filter, and the supernatant was measured by spectrophotometer.

3.5 Characterization

Morphology of the synthesized products was observed by scanning electron microscopy (SEM) and transmission electron microscope (TEM). The elements and structures of the synthesized products were also characterized using energy dispersive X-ray spectroscope (EDS) and an X-ray diffractometer (XRD), respectively. In addition, Fourier transform infrared spectroscopy (FT-IR) was used to analyze the functional group in the both pristine Fe-filled MWCNTs and acid treated Fe-filled and also Zetasizer was performed to characterize the zeta potential. Furthermore, UV-vis spectroscopy was used to measure antibiotic concentrations. The details of characterizations are presented below.

3.5.1 Scanning Electron Microscopy (SEM)

Morphology and size of the synthesized products were investigated using scanning electron microscope (SEM, JEOL: model JSM-6301F) equipped with energy dispersive X-ray spectroscopy (EDS) at National Metal and Materials Technology Center (MTEC, (shown in Figure. 3.3). The synthesized products were scattered onto adhesive carbon tapes. The specimens were placed into the sample chamber and were then operated immediately with 15 kV accelerating voltage.

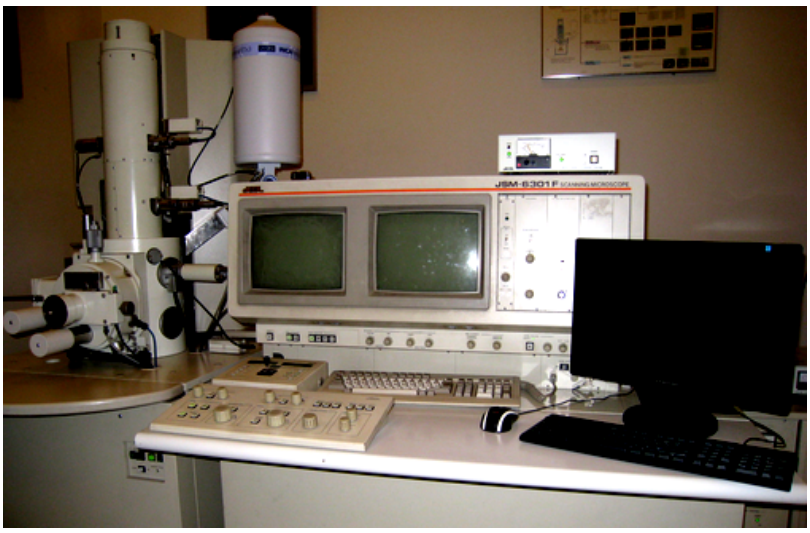

Figure 3.3 Scanning electron microscope (SEM, JEOL: model JSM-6301F)

3.5.2 Energy Dispersive X-ray Spectroscopy (EDS)

Energy dispersive X-ray spectroscope (EDS, Oxford: model INCA 350) attached to the SEM (JEOL model JSM-6301F) was used to identify elemental composition of the synthesized Fe-filled MWCNTs.

3.5.3 Transmission Electron Microscope (TEM)

Transmission electron microscope (TEM, JEOL: model JEM-2100) located at National Metal and Materials Technology Center (MTEC, (shown in Figure 3.4) was performed to analyze the structure of Fe-filled MWCNTs. The instrument was operated at 80-200 kV accelerating voltage. Before analysis, pristine Fe-filled MWCNTs and acid treated Fe-filled MWCNTs were dispersed in ethanol under an ultrasonication and the dispersion was then dropped to a copper TEM support grid.

Figure 3.4 Transmission electron microscope (TEM, JEOL model JEM-2100)

3.5.4 X-Ray Diffraction (XRD)

The structure and composition of the synthesized products were analyzed using X-ray diffraction (XRD) pattern recorded on an X-ray diffractometer (Rigaku: model TTRAX III) (shown in Figure 3.5), using Cu Kα radiation with 50 kV and 300

mA at steps of 0.02°/min in a 2θ range of 20 – 60° for analysis of synthesized products from co-pyrolysis method but using Cu Kα radiation with 40 kV and 40 mA at steps of 0.02°/min in a 2θ range of 20–80° for analysis of synthesized products from co-precipitation method.

Figure 3.5 X-ray diffractometer (XRD, Rigaku: model TTRAX III)

3.5.5 Fourier Transform – Infrared Spectroscopy (FT-IR)

The functional groups of pristine Fe-filled MWCNTs and acid treated Fe-filled MWCNTs were determined using a Fourier transform-infrared spectroscopy (FT-IR, Thermo Scientific: model Nicolet 6700) located at Center of Excellence in Particle and Technology Engineering laboratory, Chulalongkorn University (shown in Figure 3.6). The spectra were recorded on wave number between 500 and 4000 cm^{-1} with 2 cm^{-1} resolution and100 scanning for the measurement.

Figure 3.6 Fourier transform-infrared spectroscopy
(FT-IR, Thermo Scientific: model Nicolet 6700).

3.5.6 Zetasizer

The surface charge of pristine Fe-filled MWCNTs and acid treated Fe-filled MWCNTs were characterized by measurement of its zeta potential using a zetasizer (Malvern: model Nano – ZS) (shown in Figure 3.7). The measurement system was operated at 25^{o}C and 10 zeta runs. Prior to measurement, 0.1 mg of Fe-filled MWCNTs was dispersed in 10 mL de-ionized water under an ultrasonication for 3 min and then 1 ml of the dispersion was added in zeta cell. Moreover, autotitrator was connected to the zetasizer to study the effect of a change in samples pH. This instrument located at National Metal and Materials Technology Center (MTEC).

Figure 3.7 Zetasizer (Malvern, Nano – ZS: model ZEN 3500)

3.5.7 pH Meter

The pH measurements of antibiotic solutions were measured by using the pH meter (Mettler Toledo: Five Easy model FE20) (shown in Figure 3.8) which located at Excellence in Particle and Technology Engineering laboratory, Chulalongkorn University.

Figure 3.8 pH meter (Mettler Toledo, Five Easy model FE20)

3.5.8 UV-visible Spectrophotometer

Antibiotic concentrations were measured by UV-vis spectrophotometer (Shimadzu: Pharma Spec model UV-1700) (shown in Figure 3.9). This instrument is located at Excellence in Particle and Technology Engineering laboratory, Chulalongkorn University.

Figure 3.9 UV-visible spectrophotometer (Shimadzu: Pharma Spec model UV-1700)

CHAPTER IV
RESULTS AND DISCUSSION

4.1 Synthesis of Fe-filled multi-walled carbon nanotubes (Fe-filled MWCNTs)

Fe-filled multi-walled carbon nanotubes (Fe-filled MWCNTs) were synthesized by co-pyrolysis of the mixture between glycerol and ferrocene in quartz tube reactor. Pyrolyzing a mixture was employed by a tubular electrical furnace with programmable heating equipment. The temperature profile in the quartz tube reactor was controlled achieving the set point of 900°C as shown in Figure 4.1.

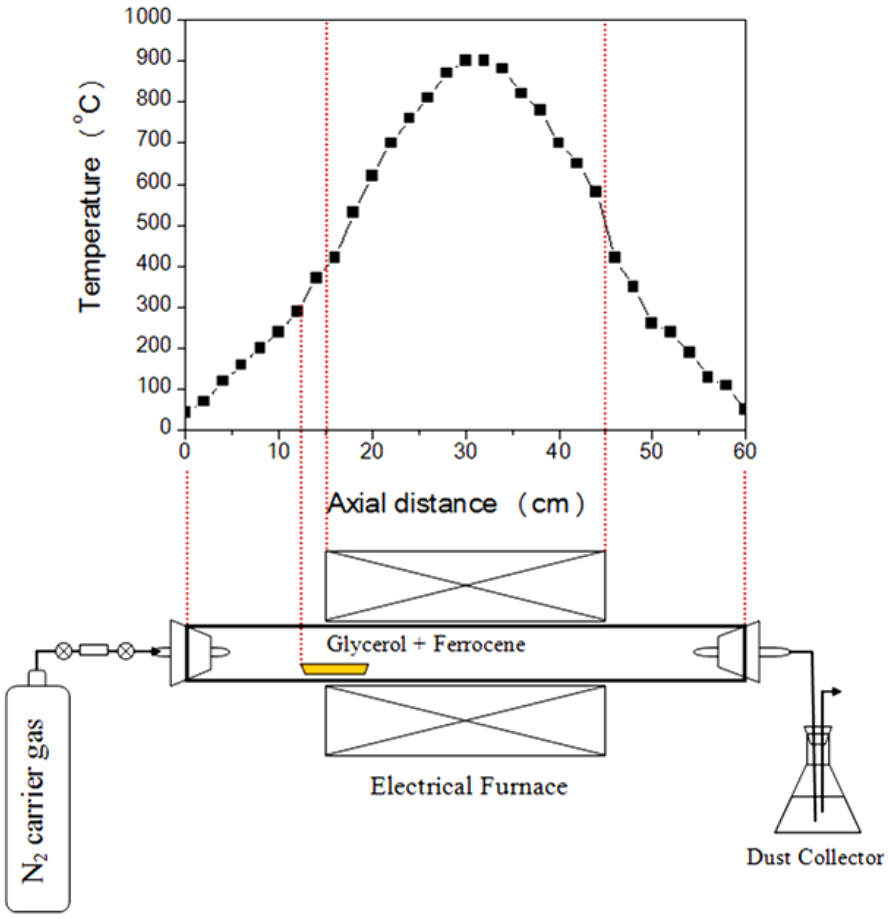

Figure 4.1 Schematic of product synthesized by co-pyrolysis and temperature distribution of the tubular reactor

The middle of the reactor exhibited a maximum temperature distribution. The mixture of glycerol and ferrocene was loaded into an alumina boat. After that, the boat of mixture was placed inside quartz tube reactor at the position of 12 cm from inlet where local temperature is able to vaporize of the mixture (300^{o}C). The vapors of the mixture were carried by nitrogen gas into the higher temperature zone. The process was operated for 30 min. Referring to temperature profiles as shown in Figure 4.1, it consisted of 3 temperature gradients along flow direction which could be clearly seen in each profile. Therefore, the collecting of the synthesized black film-like product on inner wall of quartz tube reactor was separated depending on the temperature gradient, including begin zone (0 – 20 cm from inlet) where the temperature increased from the lowest to the highest, middle zone (20 – 40 cm from inlet) where the temperature was the highest, and end zone (40 – 60 cm from inlet) where the temperature decreased from the highest to the lowest. The SEM, TEM, EDX, XRD, FT-IR and also zeta potential analysis have been used to analyze the synthesized product.

4.1.1 Morphology analysis of the synthesized products

Scanning electron microscope (SEM) and transmission electron microscope (TEM) were employed to observe morphology of all synthesized products. Based on SEM images, the as-grown product consists of large amount of carbon nanotubes (CNTs) with a few agglomeration of amorphous carbon on their surface that deposited at middle zone as shown in Figure 4.2 (b). The attained synthesized product is CNTs with outer diameter about 40 – 80 nm and several microns of length. The mainly agglomeration amorphous carbon depositing at begin zone and end zone with length of several microns and diameter in range of 45 – 200 nm, there are various particles with different morphology as shown in Figure 4.2 (a) and (c). TEM analysis revealed that those particles are multi-walled carbon nanotubes (MWCNTs), and iron clusters encapsulated in carbon shell are clearly seen.

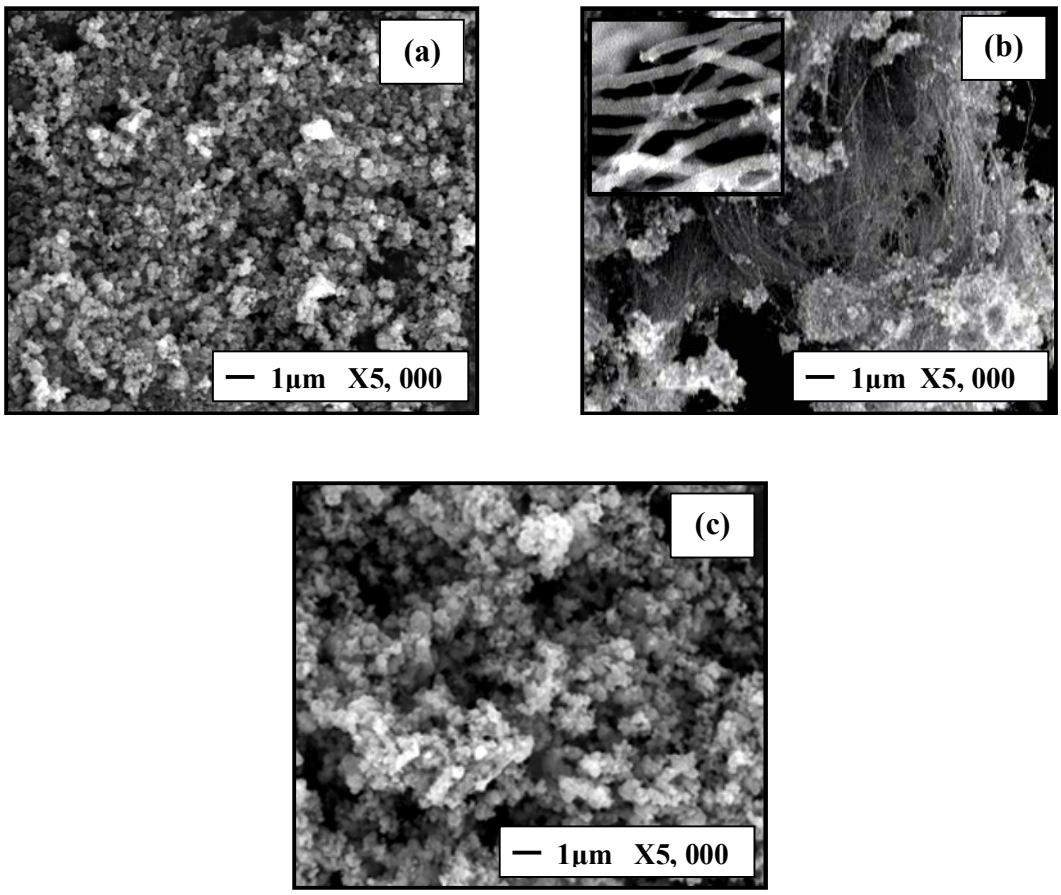

Figure 4.2 Typical SEM images of the synthesized product at different collecting zone: begin zone (a), middle zone (b) and end zone (c)

For further observation of morphology of the synthesized product, CNTs synthesized at middle zone was carefully dispersed in ethanol under ultrasonication before dropping on a copper grid for TEM analysis. As shown in Figure 4.3 (a), most of the particles structures are CNTs with outer diameter range of 40 – 80 nm and inner diameter range of 10 – 30 nm. Furthermore, clearly observed were the iron particles filled in the tube and also amorphous carbon covered on the walls of the tubes. These results are in good agreement with the SEM observation.

Higher magnification TEM image of MWCNTs as shown in Figure 4.3 (b) revealed that these Fe-filled MWCNTs are produced from the growth of carbon atoms persuaded by iron clusters catalytic. As also synthesized by Chrinpanitkul et al. (2009) [26], the condensation of iron cluster catalyst emitted from the decomposition of ferrocene leading to carbon shell would take place formation [26]. On account of

the presence of iron clusters within structure of these MWCNTs would exhibit a good respond to magnetic field.

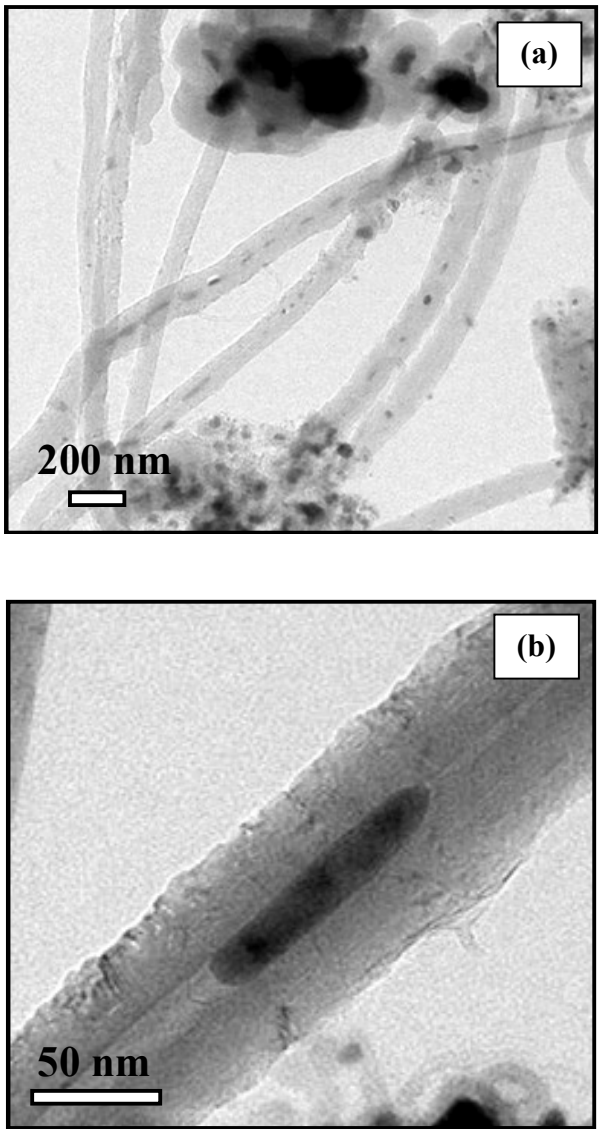

Figure 4.3 Typical TEM images of Fe-filled MWCNTs, which deposited at middle zone: the low magnification image (a) and higher magnification image (b)

4.1.2 Elemental analysis of the synthesized products

Fe-filled MWCNTs were analyzed by energy dispersive X-ray spectroscopy (EDS) for their elemental analysis as shown Figure 4.4. From the results, it is found that the synthesized product at the middle zone composed mainly of carbon (86.59 wt

%), O (7.58 wt %) and Fe (5.83 wt %). It could confirm that the synthesized product contains iron particles.

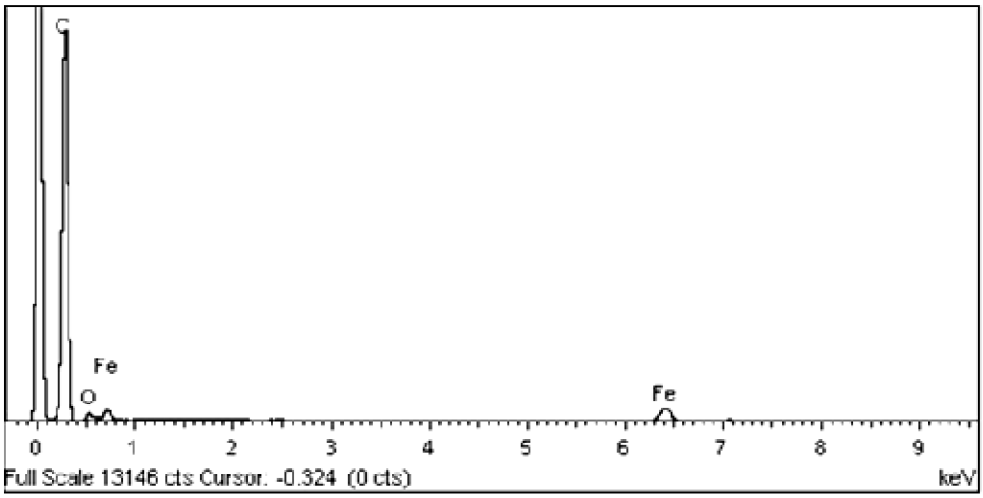

Figure 4.4 EDS spectrum of Fe-filled MWCNTs which deposited at the middle zone

XRD patterns shown in Figure 4.5 reveal the structure and chemical composition of the synthesized products. The X-ray diffraction peak at 26.1^{o} could be assigned to (002) plane of hexagonal graphite structure while another peak at 43.2^{o} suggesting that iron nanoparticles exhibit the (111) plane of the fcc (γ-Fe). In addition, it could be observed the existence of Fe with other different crystal structures such as (110) plane of the bcc (α-Fe) at 44.5^{o} [25]. Moreover, orthorhombic cementite Fe_3C phase is also observed in the XRD pattern.

Based on Fe-C phase diagram as shown in Appendix A, it could be distinctly seen that γ-Fe (in γ phase and γ + Fe_3C phase) were mainly transformed into α-Fe during the cooling down phase because α-Fe is the thermodynamically stable phase at room temperature [25]. This phenomenon was consistent with the appearance of small fraction of the γ-Fe in the XRD patterns as shown in Figure 4.5 compared to the α-Fe. While the Fe_3C is not stable at high temperature, therefore, the decomposition of the carbide into α-Fe and C atoms was happen, leading to the precipitation of the C atoms to form the CNTs at the surface of the Fe particles.

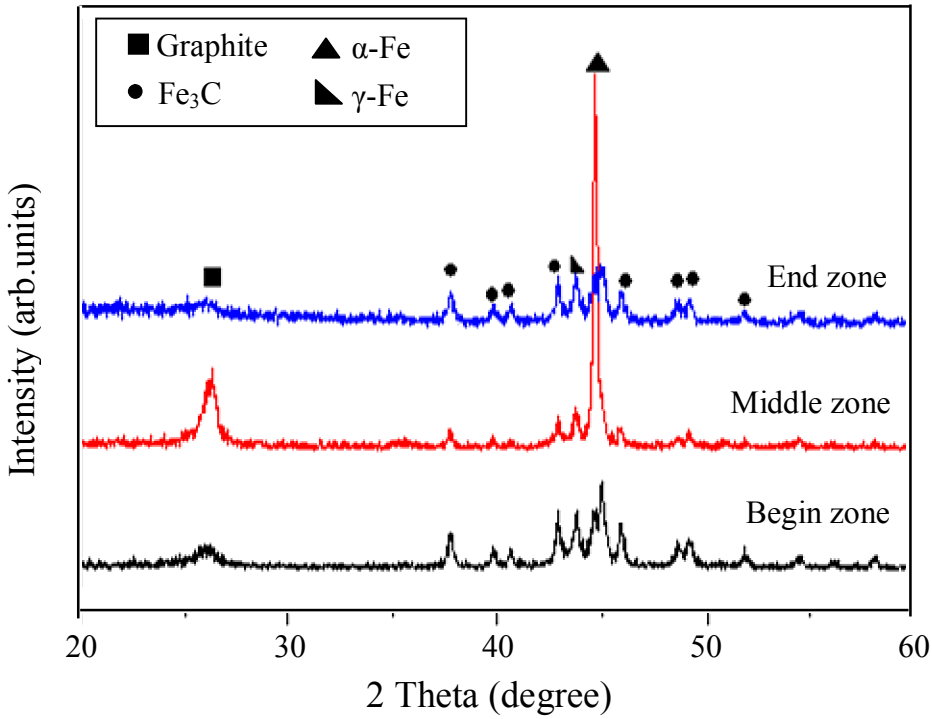

Figure 4.5 XRD patterns of the synthesized product at different collecting zone including begin zone, middle zone and end zone

4.2 Acid treatment of the synthesized Fe-filled MWCNTs

The Fe-filled MWCNTs which deposited at the middle zone were treated by acid treatment to remove impurities and also to modify the surface. The pre-determined amount of the synthesized Fe-filled MWCNTs were dispersed the mixture of concentrated nitric acid (HNO_3) and sulfuric acid (H_2SO_4).

4.2.1 Morphology analysis of acid-treated of Fe-filled MWCNTs

Figure 4.6 shows SEM images of Fe-filled MWCNTs both before and after acid treatment. In all cases, that the product under investigation are predominantly Fe-filled MWCNTs. However, it also contains amorphous carbon covered onto the side-walls. The presence of amorphous carbon are possibly a component of Fe-filled MWCNTs and, thus, intrinsic to the surface chemistry of the Fe-filled MWCNTs. More detailed, high magnification TEM images that compare the effect of acid

oxidative treatment on the Fe-filled MWCNTs structure and surface-bound amorphous carbon content can be found.

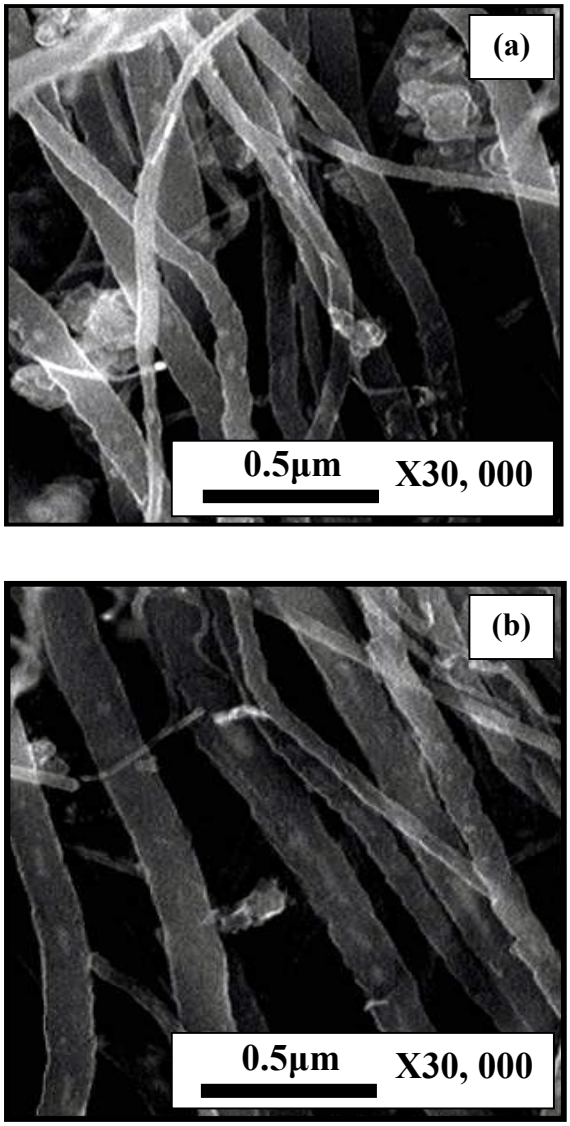

Figure 4.6 Typical SEM images of pristine Fe-filled MWCNTs (a) and acid treated Fe-filled MWCNTs (b)

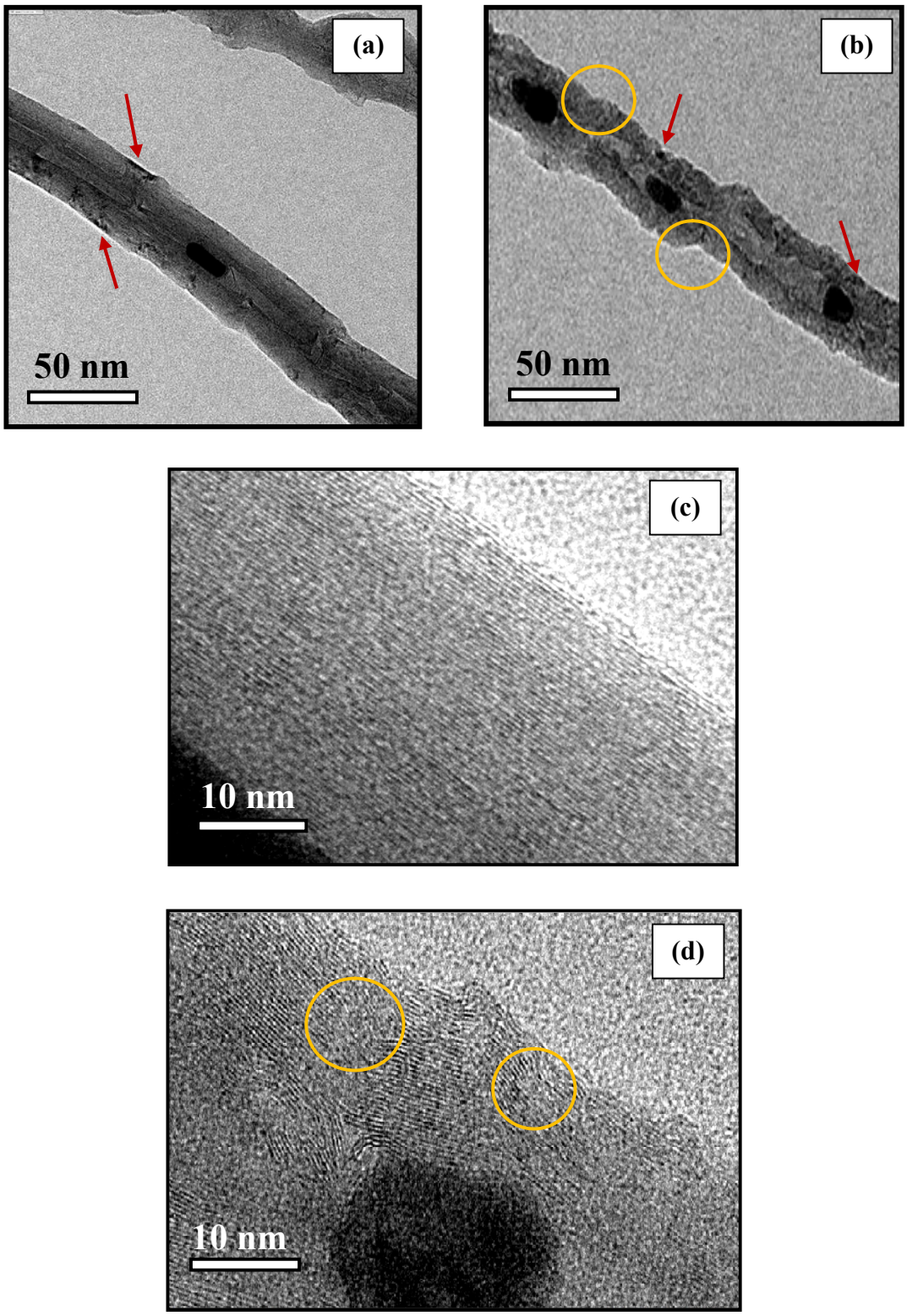

Figure 4.7 Typical TEM images with low magnification: pristine Fe-filled MWCNTs (a) and acid treated Fe-filled MWCNTs (b), with higher magnification: pristine Fe-filled MWCNTs (c) and acid treated Fe-filled MWCNTs (d)

From TEM images, it is possible to assess the number of walls, relating to detect sites in the Fe-filled MWCNTs side-walls, as well as the presence of adsorbed amorphous carbon. TEM images of pristine Fe-filled MWCNTs and Fe-filled MWCNTs that were treated by H_2SO_4/HNO_3 are shown in Figure 4.7. For the pristine Fe-filled MWCNTs, TEM images show that their outermost walls were long and straight, and also were wrapped with the presence of amorphous carbon (marked with arrows in Figure 4.7 (a)) Furthermore, parallel graphene planes oriented along the tube axis could be observed by higher magnification (see in Figure 4.7 (c)). In contrast, treatment with H_2SO_4/HNO_3 resulted in a distortion in the linearity of Fe-filled MWCNTs structure (marked with circles) and also graphene planes did not uniformly parallel as shown in Figure 4.7 (b) and (d). In some case, the outermost graphene sheet and the underlying sidewalls was extended well beyond, due to the fact that the curvature of the CNTs is sensitive from the intrinsic reactivity of the sidewall carbon atoms as well as the defect density [33].

4.2.2 Surface chemistry analysis of acid-treated of Fe-filled MWCNTs

The FT-IR spectra of pristine Fe-filled MWCNTs and acid-treated Fe-filled MWCNTs are shown in Figure 4.8. The pristine Fe-filled MWCNTs exhibited the peak at 3430 cm^{-1}, corresponding to asymmetric stretching vibration of the –OH group from carboxyl groups (O=C−OH and C−OH), while the detectable transmission band at 1578 $cm^{-1}$and 1210 cm^{-1} are assigned to the carbon skeleton [34]. In contrast, after H_2SO_4/HNO_3 treatment, the peak corresponding to a new functional group was observed at 1721 cm^{-1}, which attributed to the carbonyl group (−C=O) from carboxylic acid (-COOH) [35], which did not present in the spectra of pristine Fe-filled MWCNTs. The FT-IR spectra indicated that H_2SO_4/HNO_3 treatment generated more oxygen-containing functional groups on the outmost surfaces and defect sites, thereby improving hydrophilicity and altering negatively charged on their surface.

.

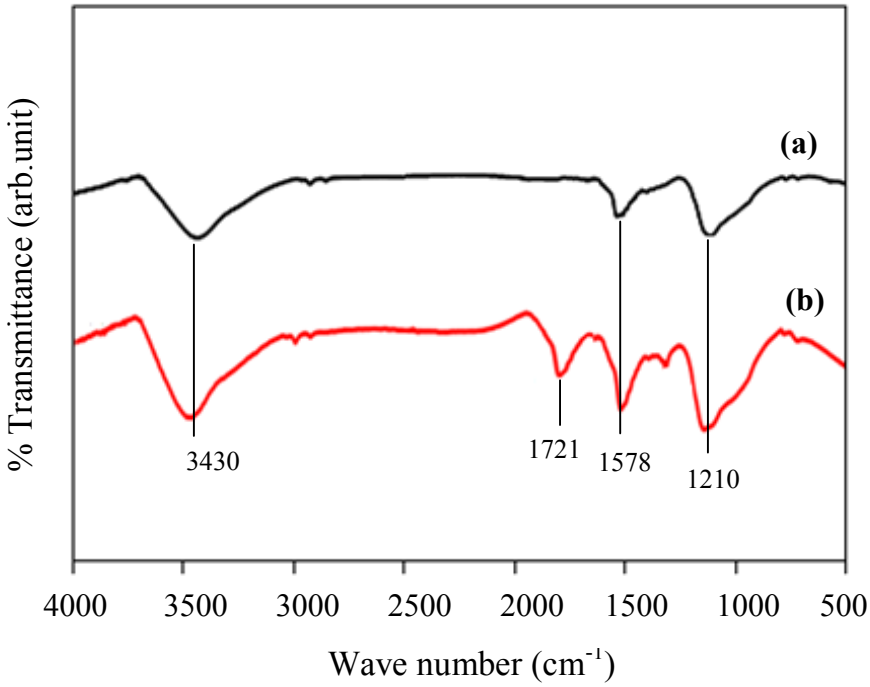

Figure 4.8 FT-IR spectra of pristine Fe-filled MWCNTs (a) and acid treated Fe-filled MWCNTs (b)

Zeta potentials were used to investigate the surface charge of Fe-filled MWCNTs before and after acid treatment suspension as shown in Figure 4.9. The point of zero charge (pH_{pzc}) of pristine Fe-filled MWCNTs and acid-treated Fe-filled MWCNTs were at pH 7.18 and 3.71, respectively, which is consistent with previous studies [36, 37]. Acid-treated Fe-filled MWCNTs could increase the amount of the oxygen-containing functional group on the surface of pristine Fe-filled MWCNTs, thus leading to lower zeta potentials of acid-treated Fe-filled MWCNTs [37].

The changes in zeta potential values might be attributed to the acid treatment of Fe-filled MWCNTs, which introduces the carboxyl groups onto their surface. The result was consistent with that observed from FT-IR. Moreover, the more negative zeta potential values of acid-treated Fe-filled MWCNTs dispersions exhibit their considerable stabilities. Previously reported study on acid functionalized SWCNTs revealed that the obtainment of stable dispersion of CNTs in water is due to the formation of electrical double layer in which ionic accumulation of few angstrom

thicknesses prevents the particle aggregation and, thereby, stabilizes the suspension [38].

In this work, the carboxyl groups on the surfaces of acid treated Fe-filled MWCNTs lead to the formation of electrical double layer around the acid treated Fe-filled MWCNTs, preventing their aggregation.

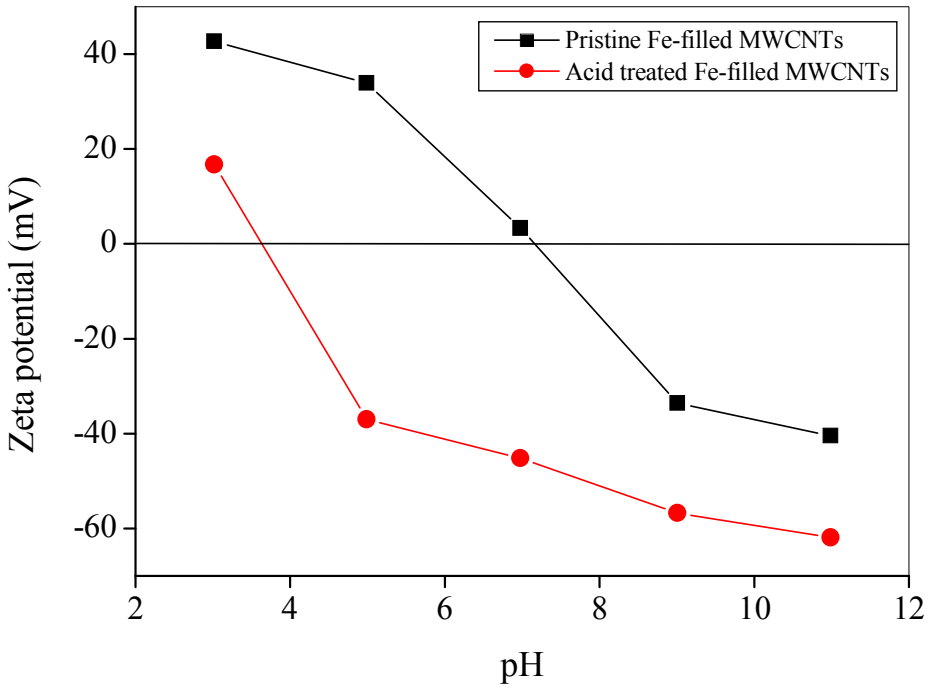

Figure 4.9 Zeta potential of Fe-filled MWCNTs as a function of pH values: (■) pristine Fe-filled MWCNTs and (●) acid treated Fe-filled MWCNTs

4.3 Synthesis of magnetic multi-walled carbon nanotubes (M-MWCNTs)

The morphology of acid-treated MWCNTs and the prepared M-MWCNTs were observed by TEM as shown in Figure 4.10 (a) and (b), respectively. The acid-treated MWCNTs by nitric acid and sulfuric acid could confirm that there were no amorphous particles remaining in the acid-treated MWCNTs. In addition, the prepared M-MWCNTs could be obviously observed that iron oxide nanoparticles (marked with arrows) were well dispersed on the surface of MWCNTs.

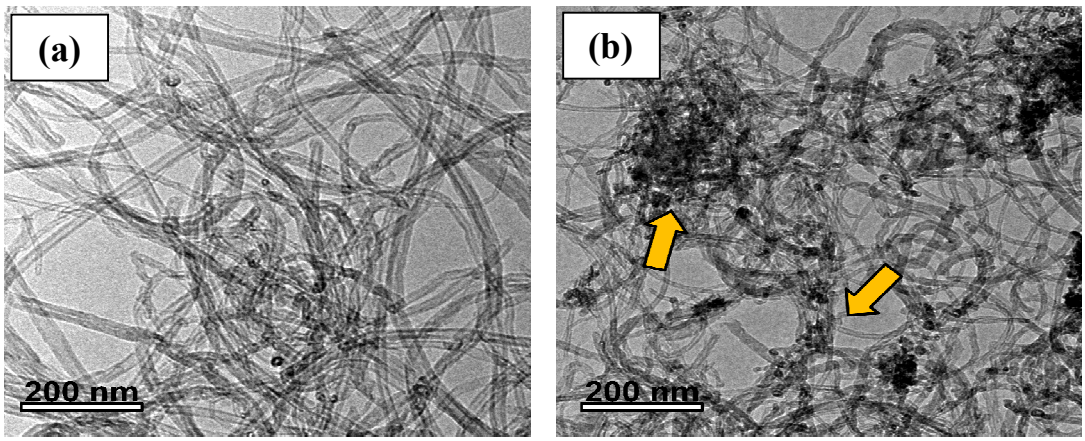

Figure 4.10 Typical TEM images of acid-treated MWCNTs (a) and M-MWCNTs (b)

The structure and chemical composition of the acid-treated MWCNTs and the synthesized M-MWCNT were revealed by XRD patterns as shown in Figure 4.11. The two diffraction peaks at 2θ = 26.18 and 43.28 in Figure 4.11 (a) could be assigned to planes of MWCNTs. There were no detectable peaks of other metallic materials or amorphous compounds within the acid-treated MWCNTs. After surfaces of acid treated MWCNTs decorated with iron oxide particles following with in situ co-precipitation, four diffraction peaks at 2θ = 30.18°, 35.78°, 43.28° and 57.48° as illustrated in Figure 4.11 (b) could be suggested to some representative of iron oxide species, which could be indexed to magnetite and maghemite that is consistent with Oliveira et al. [41]. Moreover, other minor representative peaks at 2θ = 53.78° and 62.88° may be assigned to the presence of hematite that reported with Legodi et al. [42].

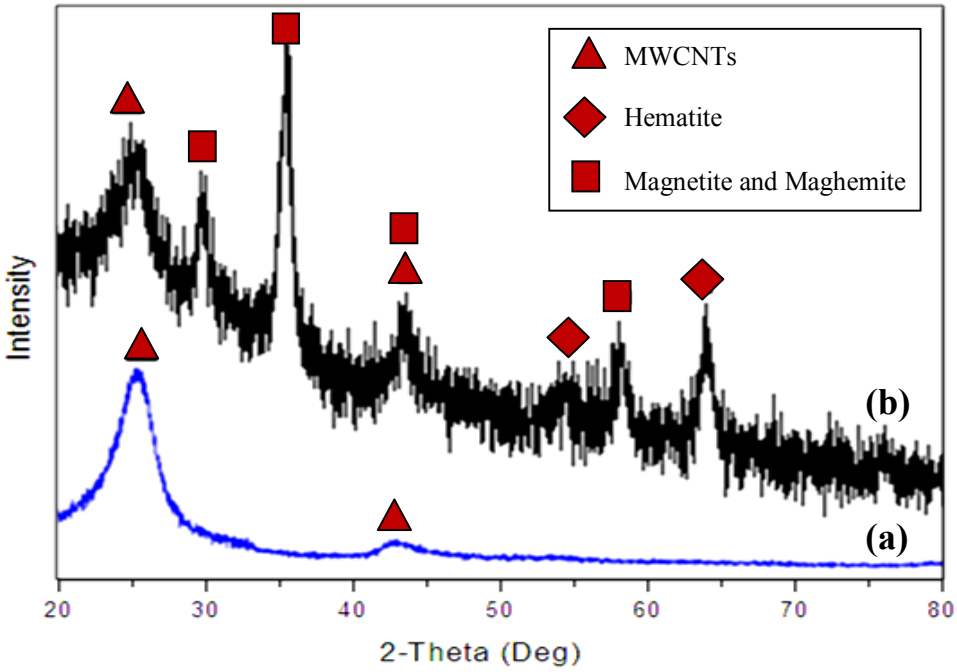

Figure 4.11 XRD patterns of acid-treated MWCNTs (a) and M-MWCNTs (b)

For the actual application, response of dried samples of the acid-treated MWCNTs and M-MWCNTs with respect to a permanent cobalt magnet was examined as demonstrated in Figure 4.12 (a) and (b). The acid-treated MWCNTs were not responsive to the cobalt magnet (Figure 4.12 (a)) but the M-MWCNTs could easily be collected within few minutes when approaching the permanent cobalt magnet near the sample bottle wall (Figure 4.12 (b)). These results may confirm that those iron oxide species could enhance the magnetic behavior of M-MWCNTs.

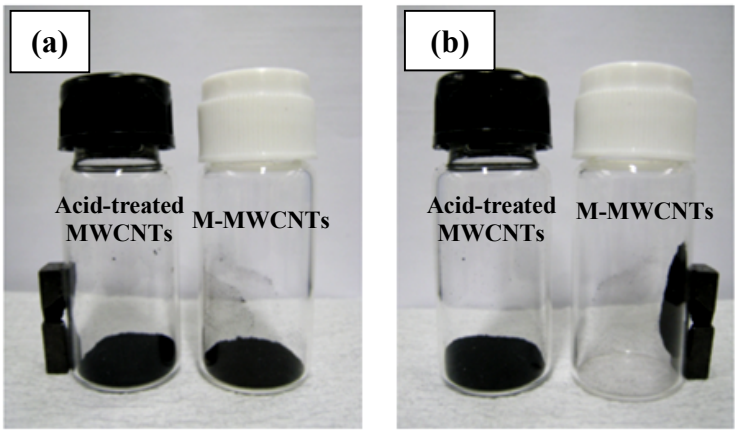

Figure 4.12 Photographs of behavior with cobalt magnet separation of acid-treated (a) and M-MWCNTs (b)

4.4 Adsorption experiments

The aim of this study was to evaluate adsorption of antibiotics (tetracycline (TTC) and enrofloxacin (ENR)) from aqueous solution using the synthesized Fe-filled MWCNTs. Aqueous solution of tetracycline (TTC, ≥95% purity, Sigma Aldrich Co.) and Enrofloxacin (ENR, ≥98% purity, Sigma Aldrich Co) were used for all batch adsorption experiments. All batch adsorption experiments were performed with a UV-vis spectrophotometer. Tetracycline concentrations were determined at maximum absorbance wavelength of 356 nm, 357 nm, 359 nm, 361 nm and 376 nm for pH 3, 5, 7, 9 and 10, respectively, enrofloxacin were determined at maximum absorbance wavelength of 316 nm, 322 nm, 323 nm and 335 nm for pH 3, 5, 7 and 10, respectively. The pH of the antibiotic solutions was adjusted by adding concentrated HCl or NaOH solution. The amount of antibiotics adsorbed on Fe-filled MWCNTs at a certain time (Q_t (mg/g)) was calculated following:

$$Q_t = (\frac{C_0 - C_t}{M}) \times V, \tag{4.1}$$

Where C_0 (mg/L) is the initial concentration of antibiotics, C_t (mg/L) is the concentration of antibiotic at a certain time t (min), V is the volume of solution (L) and M is the mass of the Fe-filled MWCNTs (g).

The adsorption efficiency of antibiotics by Fe-filled MWCNTs is defined according to equation 4.2

$$Adsorption\ efficiency = (\frac{C_0 - C_t}{C_0}) \times 100, \tag{4.2}$$

C_0 and C_t are the concentration of antibiotic at initial time and certain time (mg/L), respectively.

4.4.1 Effect of adsorbent loading studies

4.4.1.1 The amount of adsorbent loading

In order to obtain the optimal amount of adsorbent for the adsorption of antibiotics which is an important parameter in determination of adsorption capacity, the adsorption experiments were investigated in the range from 4 – 12 mg of pristine Fe-filled MWCNTs to series flasks containing 25 mL with a constant of initial antibiotic solutions of 30 mg/L and initial pH at 7.0 ± 0.5. In addition, the flasks were stirred at constant stirring for 24 hr to ensure complete equilibrium and also temperature of system was kept at 25^{o}C ± 0.5.

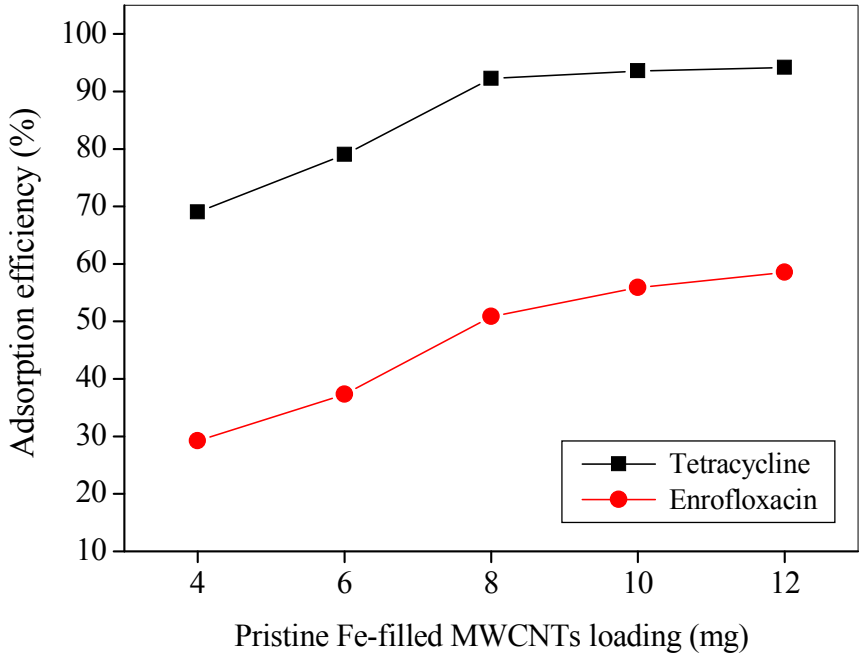

Figure 4.13 Effect of pristine Fe-filled MWCNTs loading on the adsorption of antibiotics: (■) Tetracycline and (●) Enrofloxacin

The measured results shown in Figure 4.13, represent the adsorption efficiency increased with increasing of the amount of Fe-filled MWCNTs. However, the adsorption percentage was not significantly altered beyond pristine Fe-filled MWCNTs loading of 8.0 mg. Therefore, 8.0 mg of pristine Fe-filled MWCNTs was the optimum amount of loading for the adsorption of antibiotic. From the result, it

suggested that increasing the adsorbent loading intensify the available active site on surface, leading to the increase of the adsorption on the available adsorbent surface. Although increasing of adsorbent that increases the active sites of adsorption, the increasing of the adsorbent loading might increase the possibility of the entanglement and agglomeration of the adsorbent, bringing about the decrease of the adsorption on the overlapped external surface. Based on these results, the amount of adsorbent was kept constant at 8.0 mg per 25 mL of solution, which would be conducted in further investigation.

4.4.1.2 Type of adsorbents loading

The maximum adsorption efficiency of tetracycline onto pristine Fe-filled MWCNTs, acid treated Fe-filled MWCNTs and M-MWCNTs was compared. The experiments were conducted in series flasks containing 25 mL with a constant of tetracycline solutions of 30 mg/L and initial pH at 7.0 ± 0.5 and also a temperature of system was controlled at 25^{o}C ± 0.5, stirring for 24 hr. In these experiments, 8.0 mg of precisely weighed amounts of pristine Fe-filled MWCNTs and acid treated Fe-filled MWCNTs were compared to adsorption efficiency study.

Table 4.1 Adsorption efficiency of tetracycline adsorbed on Fe-filled MWCNTs and M-MWCNTs at 25 °C ± 0.5 and pH = 7.0 ± 0.5

Antibiotic	**% Adsorption**		
	Fe-filled MWCNTs		M-MWCNTs
	Pristine	Acid-treated	
Tetracycline	92.22	71.46	89.11

The results shown in Table 4.1 reveal that pristine Fe-filled MWCNTs had a higher adsorption percentage than M-MWCNTs and acid treated Fe-filled MWCNTs. The difference percentage using both Fe-filled MWCNTs could be attributed to alternation of surface structure of Fe-filled MWCNTs after the acid treatment.

Besides, hydrophilic oxygen-containing functional group, including carboxyl and hydroxyl groups onto the surface of acid treated Fe-filled MWCNTs could form with a large number of water molecules though hydrogen bonding that either covers the adsorption sites, or prevents the tetracycline molecules entering the adsorption sites. The finding is consistent with that of Zhang et al. (2011) [19]. From these results, pristine Fe-filled MWCNTs were chosen to perform in further investigation.

4.4.2 Effect of initial pH

The initial pH of solution plays an important role in affecting adsorption efficiency as the degree of ionization of adsorbate and the surface charge of adsorbent. The effect of initial pH solution on adsorption efficiency experiments were conducted in a range from 3 to 10 (±0.5). The all experiments were performed 25 mL with 30 mg/L of antibiotic concentrations and 8 mg of pristine Fe-filled MWCNTs, also was kept at 25^{o}C ± 0.5, stirring for 24 hr. The results are shown in Figure 4.14.

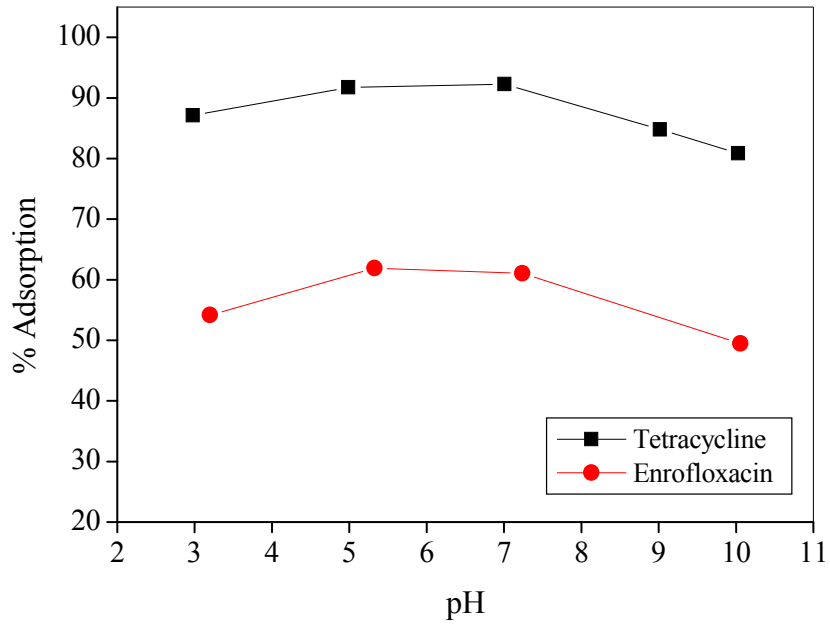

Figure 4.14 Effect of initial pH on the adsorption efficiency of antibiotics: (■) Tetracycline and (●) Enrofloxacin

For results of tetracycline adsorption, there was no change on the adsorption onto pristine Fe-filled MWCNTs with an increasing of pH from 5 – 7, the adsorption efficiency was approximately 93%. But when pH < 5 and pH > 7, the adsorption efficiency were decrease to be about 87% and 80%, respectively. These results can be explained by ionization of both the tetracycline and pristine Fe-filled MWCNTs. The protronation-deprotronation transition of functional group on pristine Fe-filled MWCNTs cannot only be affected by the variation in pH, but also result in the speciation change for ionizable organic compound [19]. Moreover, tetracycline could have different charges depending on pH solution as seen in Figure 4.15.

When solution pH is below 3.3, tetracycline exists as a cation (TCH_3^+), because of the protonation of dimethyl-ammonium group. At pH between 3.3 and 7.7, tetracycline exists as a zwitterions (TCH_2^0), because of the loss of a proton from the phenolic diketone moiety. And when solution pH is over 7.7, tetracycline exists as anion (TCH^- or TC^{2-}), due to the loss of a proton from the tri-carbonyl system and phenolic diketone moiety [20]. In this solution pH range (3.3 – 7.7), tetracycline exists as a zwitterions while the pristine Fe-filled MWCNTs surfaces are positively charged (pH_{pzc} = 7.18 as shown in Figure 4.9), on this condition, making them hardly have electrostatic attraction or repulsion mechanism. Thus the increase of pH from 5 to 7 had no significant effect on the adsorptive relation of tetracycline in this experiment. Therefore, the adsorption mechanism is probably the non-electrostatic $\pi - \pi$ dispersion interaction between bulk π systems on pristine Fe-filled MWCNTs and tetracycline molecules contained benzene rings and double bonds (C=C, C=O), or hydrophobic interaction between pristine Fe-filled MWCNTs and tetracycline [15, 19, 30].

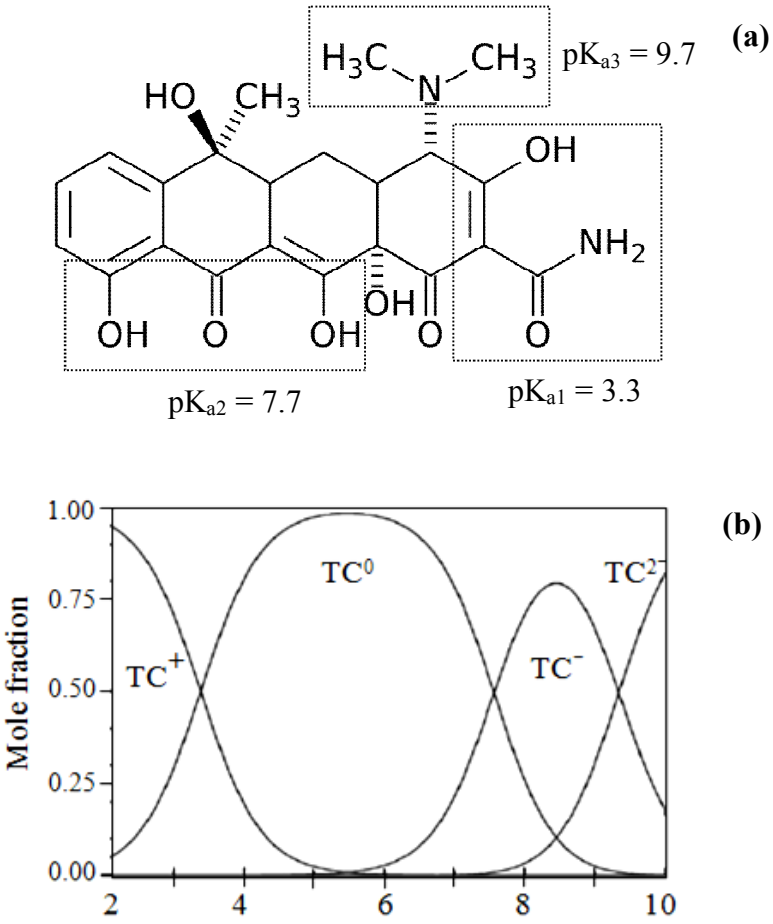

Figure 4.15 Molecular structure of tetracycline (a) and the pH-dependent speciation of tetracycline as a function of pH (b) [20]

For enrofloxacin adsorption, it was observed that the adsorption efficiency decreased when was in acidic solution and pH value increased over 8.0. The results may be explained based on the functional groups in its structure, as shown Figure 4.16, could change speciation for ionizable with variation in pH. Enrofloxacin has an acidic carboxylic group, with reported pK_a values in the 5.5 – 6.6 range, and an amino group with pK_a values for the protonated amino form in the 7.2 – 8.9 range. Based on the carboxylic acid and several basic amine functional groups, enrofloxacin is amphoteric and considered zwitterionic (ENR^0) with the pK_a values of approximately at 6.0 and 8.0 [31]. In acidic solutions, enrofloxacin is a cation ($ENRH_2^+$). And enrofloxacin is an anion (ENR^-) when the solution pH is greater than 8.0. According to these results, the mechanism for adsorption of enrofloxacin is not clear yet. The

mechanism for strong adsorption may undergo as observed in the adsorption of tetracycline onto Fe-filled MWCNTs. On the other hand, a significant decreased was observed, which may occur because enrofloxacin becomes similarly charge as the pristine Fe-filled MWCNTs causing electrostatic repulsion [19, 30].

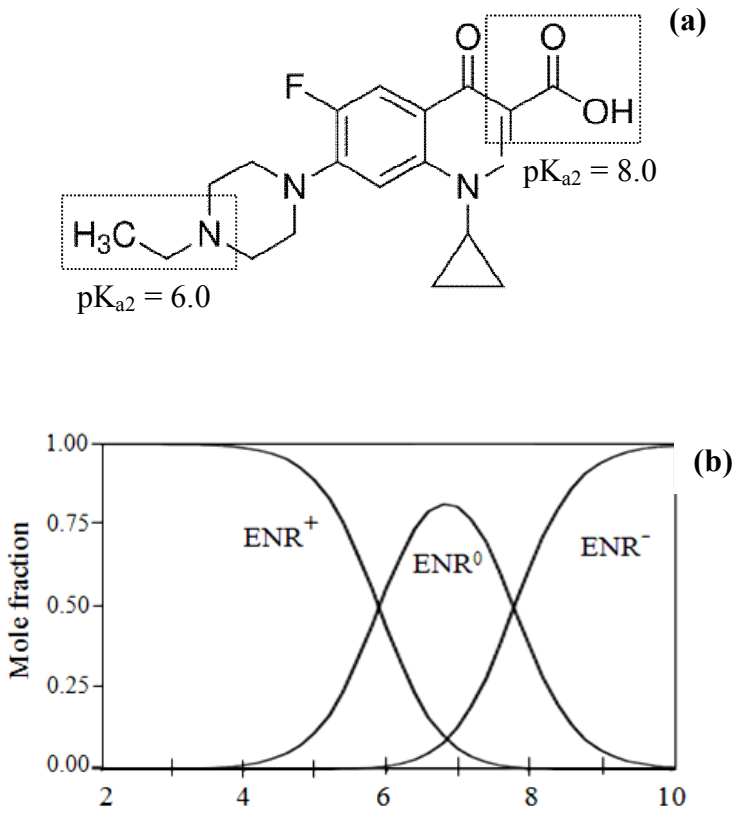

Figure 4.16 Molecular structure of enrofloxacin (a) and the pH-dependent speciation of enrofloxacinas as function of pH (b) [39]

4.4.3 Adsorption isotherms

Adsorption isotherms describe how antibiotics interact with pristine Fe-filled. To investigate the adsorption isotherms of tetracycline and enrofloxacin onto pristine Fe-filled MWCNTs at varying temperatures, batch adsorption experiments were conducted at tetracycline concentration of 10 – 100 mg/L and enrofloxacin concentration of 10 – 70 mg/L, agitating at 25, 40 and 55^{o}C for 24 hr. The equilibrium

adsorption amount of antibiotics onto pristine Fe-filled MWCNTs as a function of the equilibrium concentration of antibiotics is depicted in Figure 4.17. The measured experimental data were fitted with Langmuir and Frrundlich isotherms following Eq. (2.2) and Eq. (2.5), respectively. Plotting C_e/Q_e against C_e and log Q_e versus log C_e of the model depictions with Langmuir and Frrundlich isotherms are shown in Figure 4.18-4.19, and their calculated parameters are shown in Table 4.2. Among the adsorption isotherm models, it is found that the adsorption of tetracycline and enrofloxacin on pristine Fe-filled MWCNTs correlated well with the Langmuir isotherm model compared to the Freundlich isotherm model in all conditions.

When the temperature increased from 25°C to 55°C, the maximum adsorption capacity of tetracycline and enrofloxacin increased from 158.73 mg/g to 204.08 mg/g and 58.82 mg/g to 80.00 mg/g, respectively. It could be adsorbed to the mobility of antibiotics from solution to pristine Fe-filled MWCNTs which increased at higher temperature [30]. The essential feature of the Langmuir isotherms can be indicated by means of R_L, which a dimensionless constant referred to as the separation factor or equilibrium parameter. The calculated R_L values, shown in Table 4.2, were found to be between 0 and 1. Hence, the adsorption process was entirely favorable and the pristine Fe-filled MWCNTs employed exhibited a good potential for the adsorption of tetracycline and enrofloxacin.

Table 4.2 Adsorption isotherm parameters of antibiotics adsorbed on pristine Fe-filled MWCNTs at different temperature and pH = 7±0.5

Antibiotics	**T (°C)**	**Langmuir model**				**Freundlich model**		
		Q_m (mg/g)	K_L (L/mg)	R_L	R^2	K_F (mg/g)(L/mg)^n	n	R^2
TTC	25	158.73	0.52	0.019 – 0.158	0.9971	64.39	4.04	0.9785
	40	181.82	0.63	0.015 – 0.134	0.9984	73.52	3.75	0.9861
	55	204.08	1.23	0.008 – 0.074	0.9996	94.06	3.81	0.9725
ENR	25	58.82	0.26	0.052 – 0.277	0.9986	18.97	3.47	0.9588
	40	70.92	0.27	0.051 – 0.271	0.9997	20.37	3.04	0.9628
	55	80.00	0.28	0.048 – 0.258	0.9992	22.13	2.87	0.9509

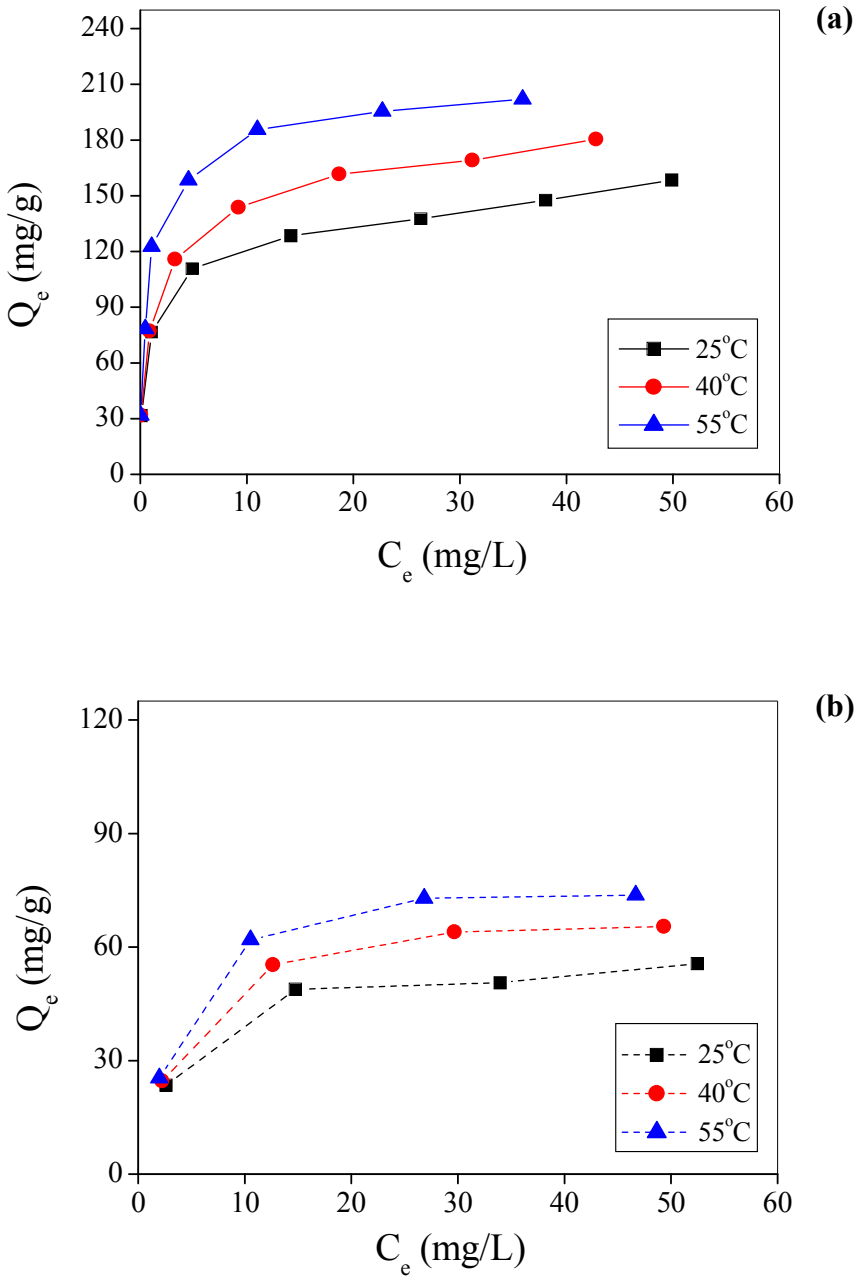

Figure 4.17 Adsorption isotherm of tetracycline (a) and enrofloxacin (b) adsorbed on pristine Fe-filled MWCNTs at pH = 7±0.5 and different temperature: (■) 25°C, (●) 40°C and (▲) 55°C

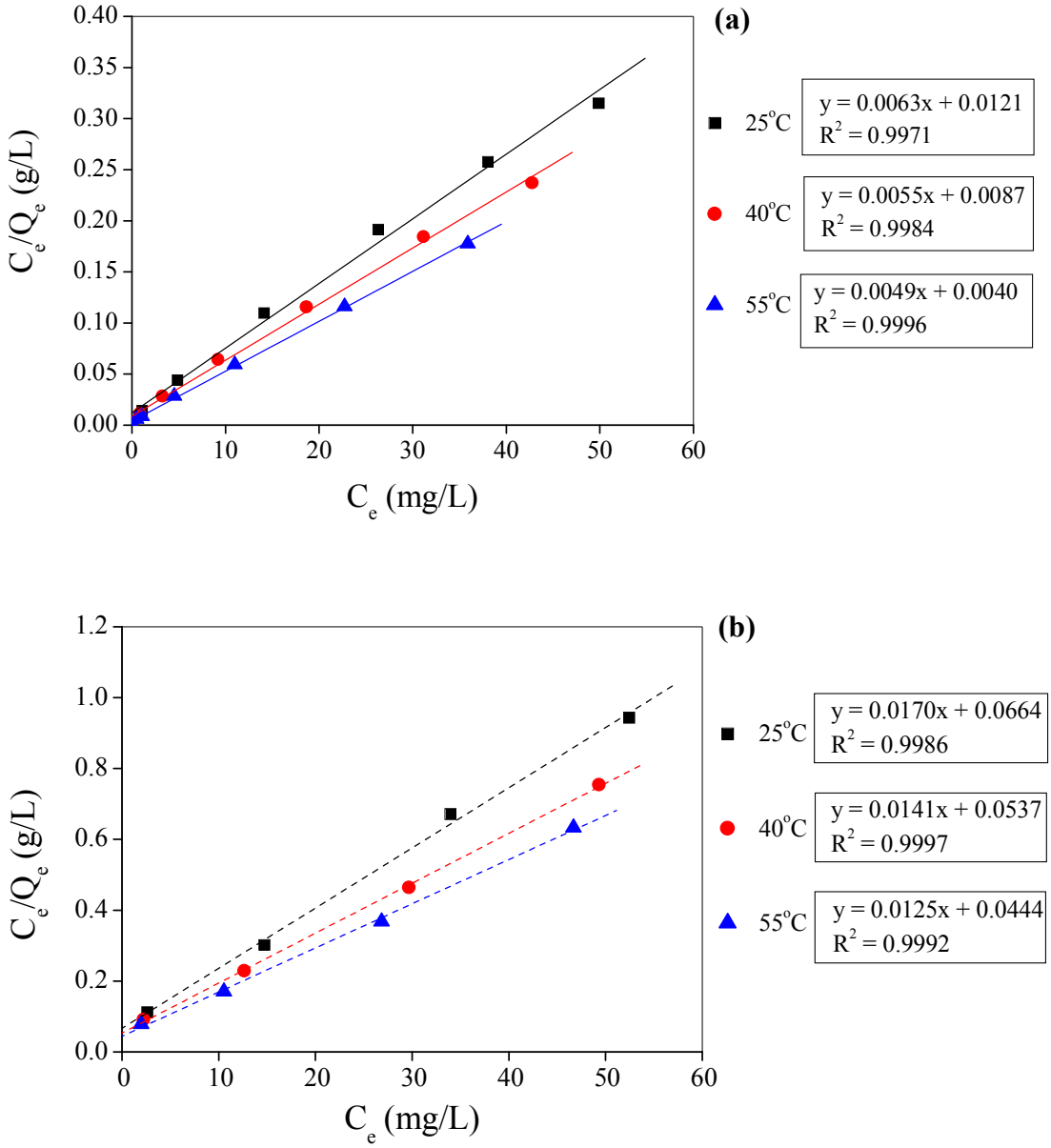

Figure 4.18 Langmuir isotherm plots for the adsorption of tetracycline (a) and enrofloxacin (b) adsorbed onto pristine Fe-filled MWCNTs at pH = 7±0.5 and different temperature: (■) 25°C, (●) 40°C and (▲) 55°C

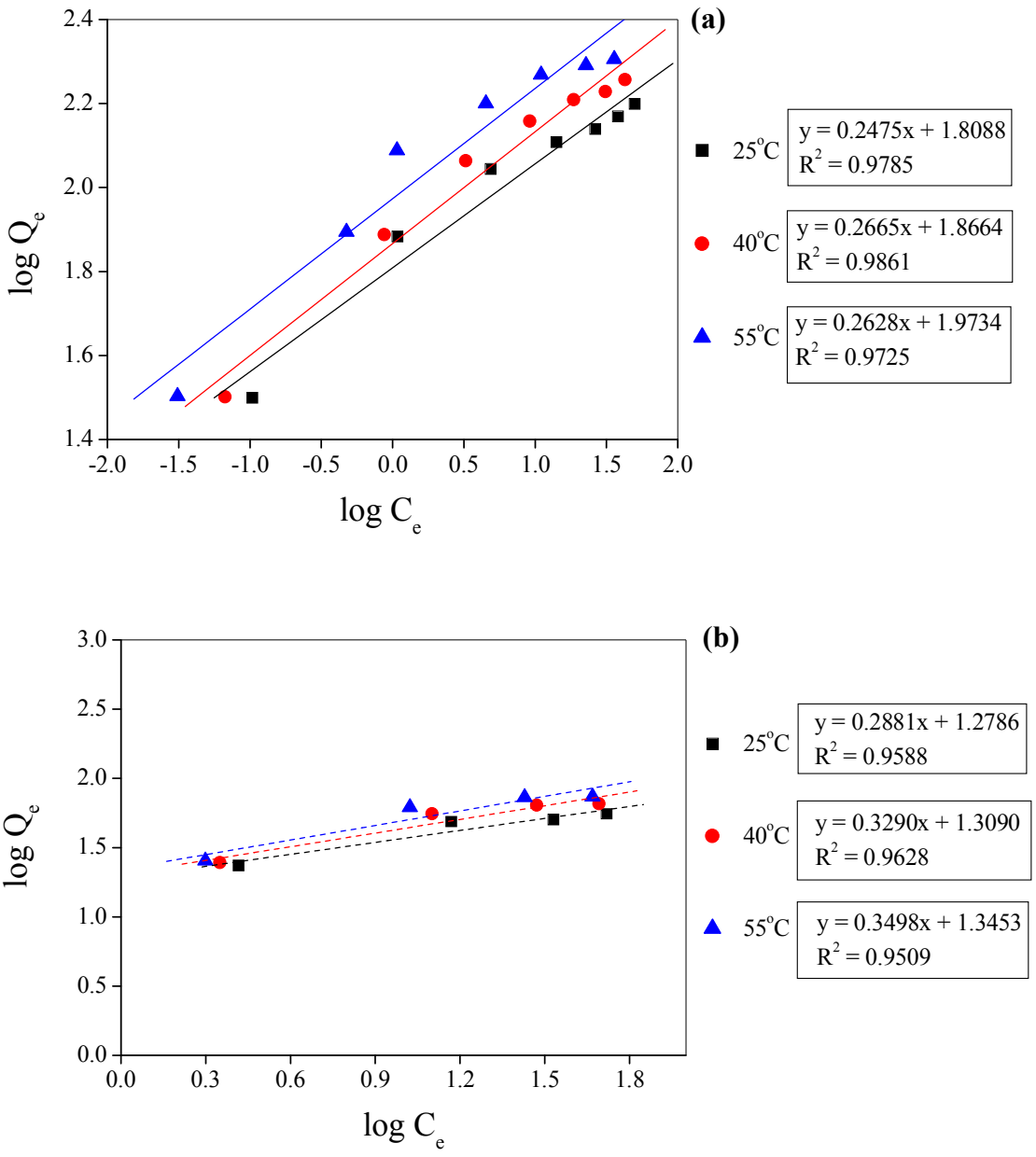

Figure 4.19 Freundlich isotherm plots for the adsorption of tetracycline (a) and enrofloxacin (b) adsorbed onto pristine Fe-filled MWCNTs at pH = 7±0.5 and different temperature: (■) 25°C, (●) 40°C and (▲) 55°C

4.4.4 Thermodynamic studies

Study of the temperature dependence of adsorption provides valuable information regarding the energetic changes during adsorption. The adsorption isotherms of tetracycline and enrofloxacin on to pristine Fe-filled MWCNTs at 25, 40, and 55°C were obtained to determine the thermodynamic parameters. The equilibrium adsorption coefficient (K_c) for the adsorption was defined as follow [40]:

$$K_C = \frac{Q_e}{C_e}, \tag{4.3}$$

where C_e is the equilibrium concentration of antibiotics and Q_e is the amount of antibiotics adsorbed per unit weight of pristine Fe-filled MWCNTs at equilibrium concentration (mm/g).

The standard Gibbs free energy change (ΔG^0), standard enthalpy change (ΔH^0), and standard entropy change (ΔS^0) were calculated from K_c by the following equation [37]:

$$\Delta G^0 = -RT \ln K_C, \tag{4.4}$$

$$\Delta G^0 = \Delta H^0 - T\Delta S^0, \tag{4.5}$$

The combination of Eq. (4.4) and (4.5) yield:

$$\ln K_C = \frac{-\Delta G^0}{RT} = \frac{\Delta S^0}{R} - \frac{\Delta H^0}{RT}, \tag{4.6}$$

where R is the universal gas constant (8.314 J/mol*K), T is the temperature (K) and K_c is the equilibrium adsorption coefficient. Gibbs free energy change of adsorption (ΔG^o) was defined using ln K_c values for different temperatures. According to Eq. (4.7), ΔH^0 and ΔS^0 parameters can be obtained from the slope and intercept of the liner plot of lnKc against 1/T in Figure 4.20.

The thermodynamic parameters are listed in Table 4.3. The positive values of ΔH^0 and the negative values of ΔG^o confirmed the endothermic and spontaneous nature of sorption process. Additionally, on the basis of relatively small enthalpy change, it can be inferred that the nature of the adsorption process for both

tetracycline and enrofloxacin is physical, either van der Waal's attraction or hydrogen bonding with the low enthalpies exchanged (below 40 kJ/mol) [31].

Table 4.3 Thermodynamic parameters of antibiotics adsorbed on pristine Fe-filled MWCNTs at different temperature and pH = 7±0.5

Antibiotics	C_0 (mg/L)	ΔG^o (kJ/mol)			ΔH^0 (kJ/mol)	ΔS^0 (KJ/mol-K)
		25°C	40°C	55°C		
TTC	100	-2.863	-3.746	-4.713	+15.492	+0.062
ENR	70	-0.145	-0.735	-1.246	+10.813	+0.036

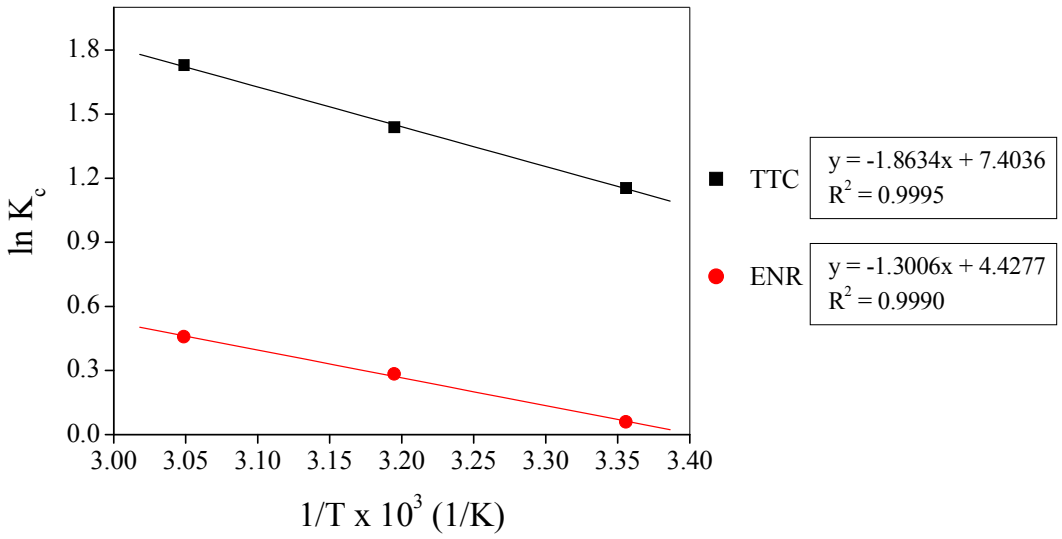

Figure 4.20 Correlation between lnK_c and 1000/T of antibiotics adsorbed onto pristine Fe-filled MWCNTs as function of temperature:
(■) Tetracycline and (●) Enrofloxacin

4.4.5 Kinetic adsorption studies

4.4.5.1 Contact time

In order to examine the influence of temperature on the uptake rate of tetracycline and enrofloxacin, the experiments were conducted at 25, 40, 55°C.

Samples were taken at regular intervals. The quantity of the amount adsorbed at time at different temperature was calculated according to Eq. (4.1). The results are depicted in Figure 4.21.

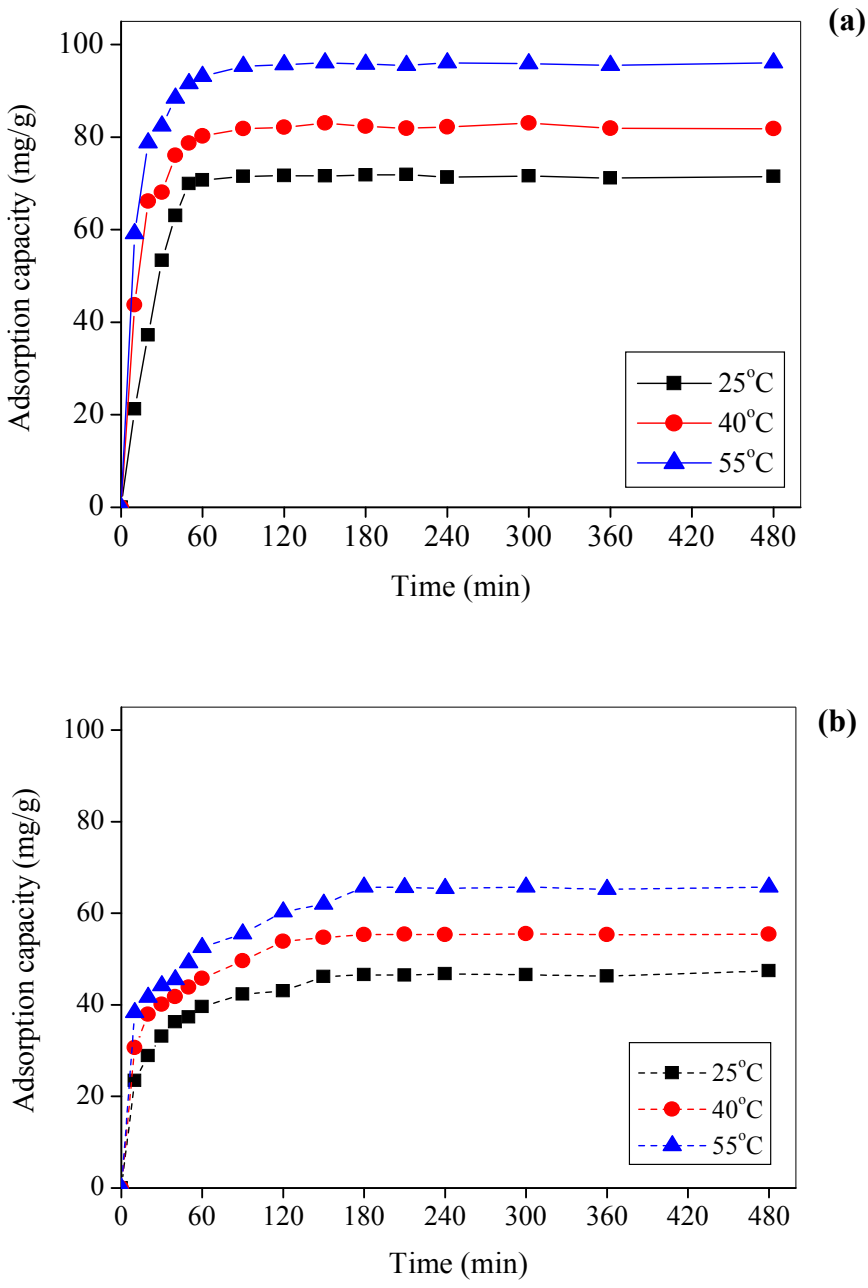

Figure 4.21 The adsorption capacity of tetracycline (a) and enrofloxacin (b), as a function of time at the different temperature: (■) 25°C, (●) 40°C and (▲) 55°C

As can be observed, the obtained curves reflect that the adsorption of tetracycline and enrofloxacin onto pristine Fe-filled MWCNTs has the similar trends. The adsorption capacity changed due to temperature indicated that higher temperatures favored both removals from aqueous solutions. In addition, the adsorption rate of tetracycline increases quickly with time and then reaches equilibrium within 1 hr while the adsorption of enrofloxcacin did not change significantly after 3 hr, which consistent with the previous studies [30, 31]. Although the adsorption capacity was increased when the temperature increased, the reaching to equilibrium of these adsorption did not change significantly.

4.4.5.2 Kinetics modeling

In order to investigate the adsorption process of tetracycline and enrofloxacin onto pristine Fe-filled MWCNTs, two common kinetics models including the pseudo-first-order and pseudo-second-order models have been used to fit the experiment data.

(a) Pseudo-first-order model

The pseudo-first-order kinetic model can be expressed following as [37]:

$$\frac{dQ_e}{dt} = k_1(Q_e - Q_t). \qquad (4.7)$$

The above equation (Eq. 4.7) is integrated for the boundary condition t = 0 to t = t and $Q_t = 0$ to $Q_t = Q_t$, it may be rearranged for straight-line data plots as shown in Eq. (4.9):

$$\ln(Q_e - Q_t) = \ln(Q_e) - k_1 t, \qquad (4.8)$$

where Q_e (mg/g) and Q_t (mg/g) are the amount of antibiotics adsorbed onto pristine Fe-filled MWCNTs at equilibrium and at time t (min), respectively, and k_1 (min^{-1}) is the rate constant of the pseudo-first-order adsorption. The values k_1 for this adsorption were determined from the plot of ln ($Q_e - Q_t$) against t.

(b) Pseudo-second-order model

The pseudo-first-order kinetic model can be expressed as follow [37]:

$$\frac{dQ_e}{dt} = k_2(Q_e - Q_t)^2 \qquad (4.9)$$

Integrating Eq. (4.10) for the boundary condition $t = 0$ to $t = t$ and $Q_t = 0$ to $Q_t = Q_t$, it can be rearranged to obtain:

$$\frac{t}{Q_t} = \frac{1}{k_2 Q_e^2} + \frac{1}{Q_e}t \qquad (4.10)$$

where k_1 (g/mg*min) is the rate constant of the pseudo-second-order adsorption. The straight-line plots of t/Q_t versus t have been determined to obtain rate parameters.

The pseudo-second-order rate constants were used to calculate the initial adsorption rate, h (mg/g*min) [19], given by Eq. (4.11):

$$h = k_2 Q_e^2. \qquad (4.11)$$

The experimental data of batch kinetic were fitted to both pseudo-first-order and pseudo-second-order models that are depicted in Figure 4.19 – 4.20. The results of the kinetic parameters and the determined initial adsorption rate values are listed in Table 4.4 – 4.5

The reliability of model fitting can be determined by the value of R^2 and comparing the values of $Q_{e,\mathrm{Exp}}$ and $Q_{e,\ \mathrm{Cal}}$. Based on the correlation coefficients of determination (R^2) of the adsorption, both tetracycline and enrofloxacin are best described by the pseudo-second-order model. In addition, all of the calculated values of $Q_{e,\ \mathrm{Exp}}$ (mg/g) values are closer to $Q_{e,\ \mathrm{Cal}}$ (mg/g) values calculated from the pseudo-second-order kinetic model. Moreover, the initial adsorption rate increased with the increase of temperature in a given adsorption system.

Table 4.4 Kinetic parameters of pseudo-first-order model for antibiotics adsorption on pristine Fe-filled MWCNT at different temperatures

Antibiotics	T (°C)	Pseudo-first-order model			
		$Q_{e,Exp}$ (mg/g)	$Q_{e,Cal}$ (mg/g)	k_1 x10^3 (min^{-1})	R^2
TTC	25	67.04	55.21	65.64	0.9947
	40	81.00	68.50	68.40	0.9927
	55	93.60	79.62	72.31	0.9938
ENR	25	47.56	29.81	19.11	0.9799
	40	56.31	35.17	20.42	0.9863
	55	66.73	48.07	21.42	0.9882

Table 4.5 Kinetic parameters of pseudo-second-order model for antibiotics adsorption on pristine Fe-filled MWCNT at different temperatures**.**

Antibiotics	T (°C)	Pseudo-second-order model				
		$Q_{e,Exp}$ (mg/g)	$Q_{e,Cal}$ (mg/g)	k_2 x 10^3 (g/mg-min)	h (mg/g-min)	R^2
TTC	25	67.04	68.49	3.40	15.95	0.9976
	40	81.00	82.64	4.52	30.86	0.9982
	55	93.60	92.59	5.28	45.25	0.9978
ENR	25	47.56	48.54	1.23	2.91	0.9970
	40	56.31	57.80	1.57	5.23	0.9967
	55	66.73	68.49	2.11	9.90	0.9974

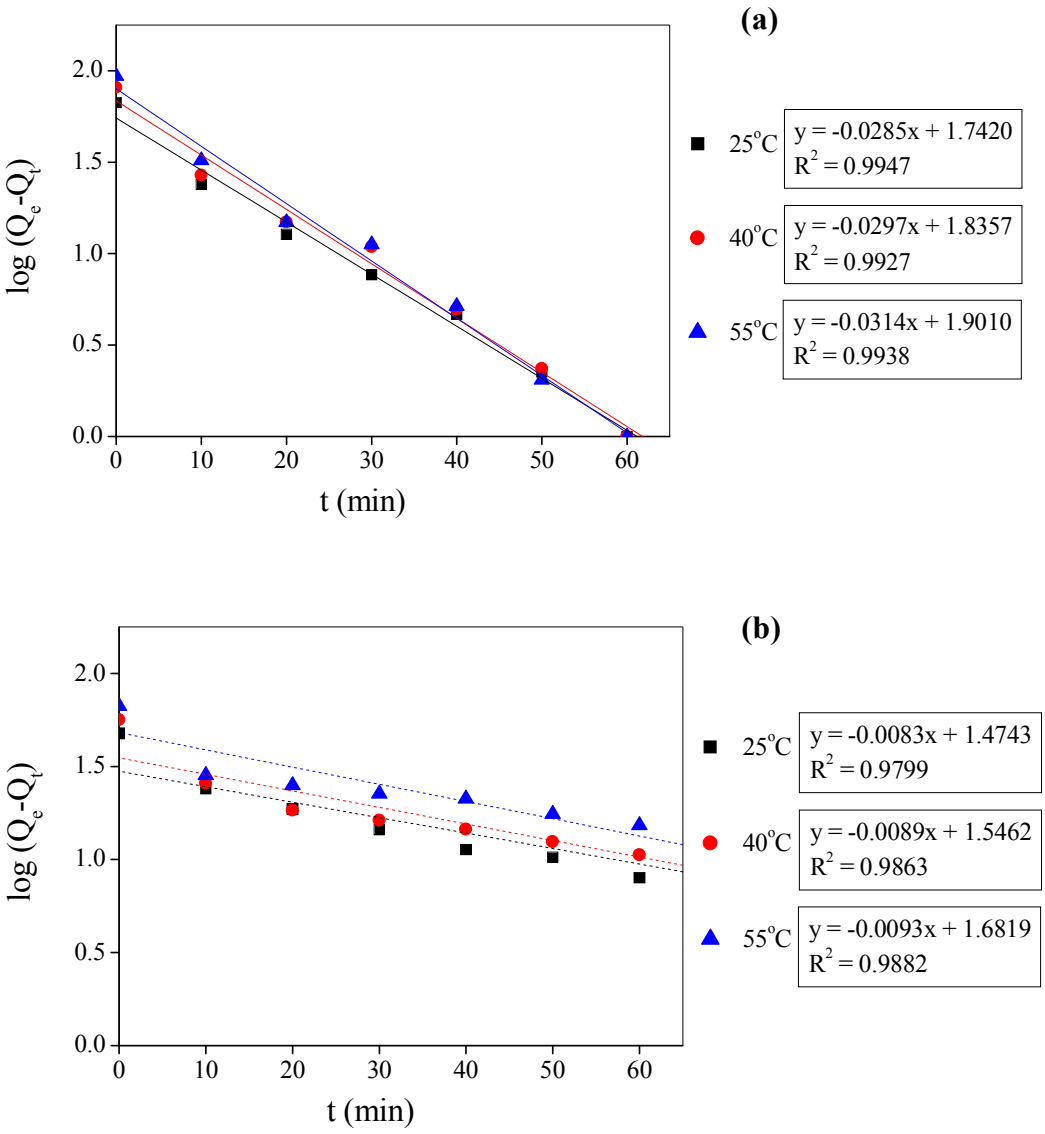

Figure 4.22 Pseudo-first-order plots for the adsorption of tetracycline (a) and enrofloxacin (b) adsorbed onto pristine Fe-filled MWCNTs at different temperature: (■) 25°C, (●) 40°C and (▲) 55°C

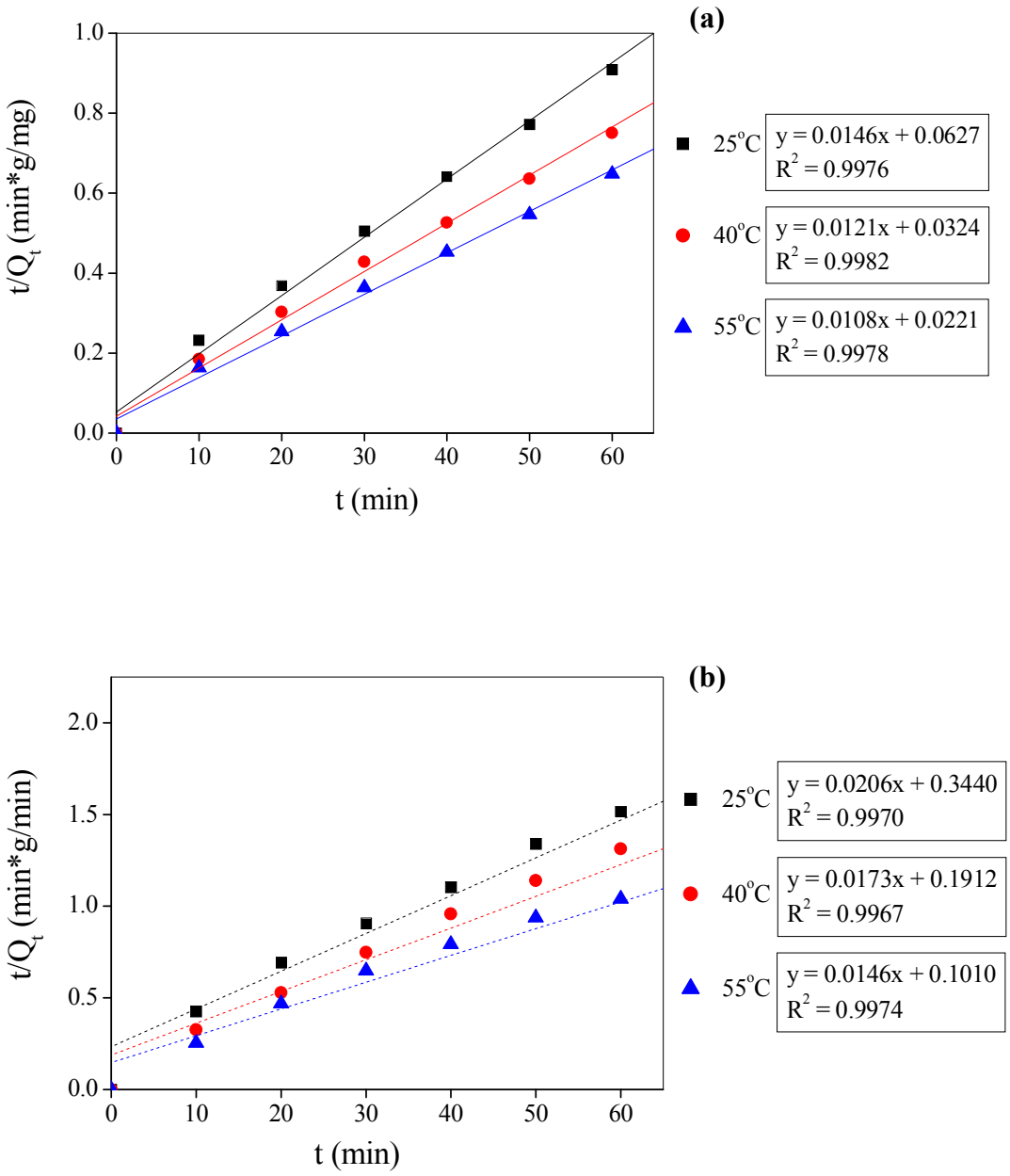

Figure 4.23 Pseudo-second-order plots for the adsorption of tetracycline (a) and enrofloxacin (b) adsorbed onto pristine Fe-filled MWCNTs at different temperature: (■) 25°C, (●) 40°C and (▲) 55°C

Furthermore, the activation energy (E_a) for adsorption was possible calculated according to the Arrhenius equation based on the obtained k_2 values in Table 4.5. Arrhenius equation [19] is as follows:

$$k = Ae^{\left(\frac{-E_a}{RT}\right)}, \tag{4.12}$$

where A is the frequency factor (min^{-1}), E_a is the activation energy (kJ /mol), R is the ideal gas constant (J/mol*K) and T is the absolute temperature (K).

Eq. (4.13) can be converted into Eq. (4.14) by taking logarithm:

$$\ln k_2 = \ln A - \frac{E_a}{RT}. \tag{4.13}$$

Thus, E_a could be determined from the slope of the line plotting ln k_2 versus 1000/T as shown in Figure 4.24. From the results, the estimated E_a for the adsorption of tetracycline and enrofloxacin onto pristine Fe-filled MWCNTs were 11.97, 14.36 kJ/mol, respectively. As the obtained, E_a of tetracycline adsorption is lower than enrofloxacin, leading to the uptake rate of tetracycline had more rapid adsorption than enrofloxacin, which is consistent with the obtained k_2 values.

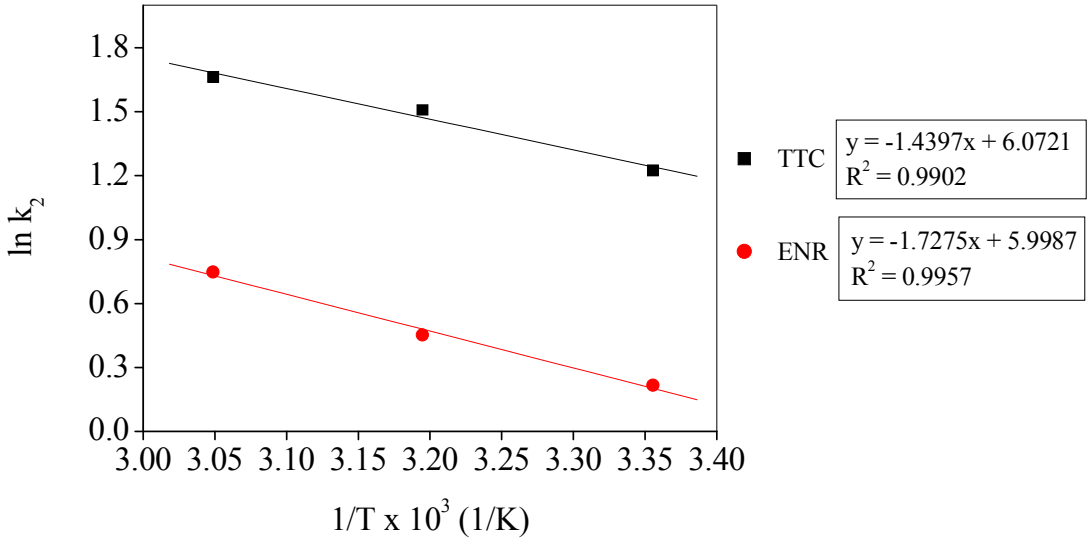

Figure 4.24 Correlation between ln k_2 and 1000/T of antibiotics adsorbed onto pristine Fe-filled MWCNTs as function of temperature:
(■) Tetracycline and (●) Enrofloxacin

4.5 Separation efficiency (%) of exhausted Fe-filled MWCNTs by magnet

The adsorption characteristics of pristine Fe-filled MWCNTs are displayed in Figure 4.22. It was observed that the pristine Fe-filled MWCNTs were fully mixed with the tetracycline solution and also could be easily separated from the aqueous solution within few minutes by placing a permanent magnet near the glass bottle.

The exhausted pristine Fe-filled MWCNTs were separated from solution and were then dried at 80°C for overnight. The dried exhausted were measured weight. After that, weight of exhausted pristine Fe-filled MWCNTs is used to calculated the weight loss which could not be separated by magnet following equation (4.13)

$$Weight\ loss\ (\%) = \frac{initial\ weight - final\ weight}{initial\ weight} \times 100 \qquad (4.13)$$

From the calculation, weight loss of exhausted pristine Fe-filled MWCNTs was merely 7.29%. It proved that pristine Fe-filled MWCNTs could be highly separated by a permanent magnet by about 92.71%.

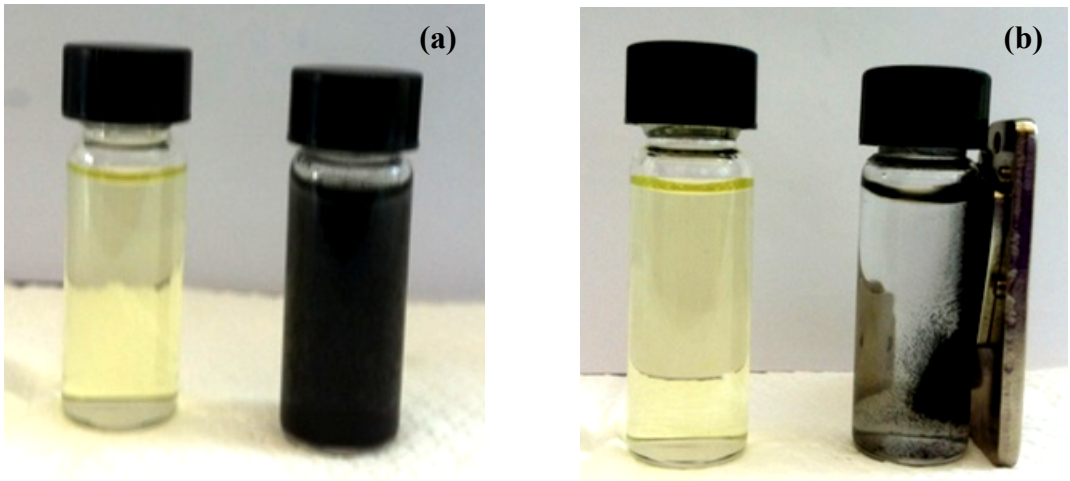

Figure 4.25 The photographs of pristine Fe-filled MWCNTs adsorption behavior and magnetic separation: TTC solution and the suspension of TTC and pristine Fe-filled MWCNTs (a) and TTC solution and separation of the pristine Fe-filled MWCNTs from solution by a magnet after 8 hr adsorption (b)

CHAPTER V

CONCLUSIONS AND RECOMMENDATION

5.1 Conclusions

In this work, Fe-filled MWCNTs were synthesized by co-pyrolysis method at 900^{o}C. Glycerol and ferrocene at molar ratio of 5: 1 were used for precursor. Nitrogen was used as carrier gas during the pyrolysis process. The process was conducted for 45 minutes. The synthesized Fe-filled MWCNTs were collected from the middle zone of the quartz tube reactor. In addition, the synthesized Fe-filled MWCNTs were treated with 3: 1 the volumetric ratio of H_2SO_4/HNO_3. Furthermore, both pristine Fe-filled MWCNTs and acid treated Fe-filled MWCNTs were carefully characterized before investigating their adsorption properties for the removal of tetracycline (TTC) and enrofloxacin (ENR). The adsorption characteristics and the effect of external factors such as pH and temperature were also investigated. The following conclusions can be made.

5.1.1 Morphology and structure of Fe-filled MWCNTs

For this synthesized condition, Fe-filled MWCNTs could be highly generated at middle zone of quartz tube reactor. The attained synthesized Fe-filled MWCNTs had inner diameter range of 10 – 30 nm, outer diameter range of 40 – 80 nm, and length of several microns. Moreover, iron particles were filled in the tube, suggesting that these Fe-filled MWCNTs are produced from the growth of atoms which are persuaded by iron clusters catalyst. The iron particles were identified as austenite (γ-Fe), ferrite (α-Fe) and iron carbide (Fe_3C). Furthermore, Fe-filled MWCNTs were treated with acid leading to a distortion in the linearity and destruction in graphene planes of their structure. At the same time, the functional group, which is the product of carbonyl group (−C=O), was produced on the Fe-filled MWCNTs surface. This functional group did not present in the FT-IR spectra of pristine Fe-filled MWCNTs. Thus, the outmost surfaces of Fe-filled could be generated more oxygen-containing functional groups by H_2SO_4/HNO_3, thereby improving hydrophilicity and altering negatively charged on their surface, also leading to lower zeta potentials.

5.1.2 The efficiency removal of antibiotic by the synthesized Fe-filled MWCNTs

In this study, the adsorption behavior of tetracycline and enrofloxacin onto the synthesized Fe-filled MWCNTs was investigated. For both pristine Fe-filled MWCNTs and acid treated Fe-filled MWCNTs, the highest adsorption efficiency of 92% for tetracycline was observed on the pristine Fe-filled MWCNTs. Besides, hydrophilic oxygen-containing functional group could form with a large number of water molecules through hydrogen bonding that may either covers the adsorption site, or prevents the tetracycline molecules entering to the adsorption sites, leading to low adsorption efficiency for the treated Fe-filled MWCNTs. The adsorption efficiency of both tetracycline and enrofloxacin onto pristine Fe-filled MWCNTs increased when pH was increased from 5 – 7 and then decreased significantly as the pH lower or higher than this range. The effect of pH was associated with the pH-dependent speciation of antibiotics (tetracycline and enrofloxacin) and the surface charge behavior of pristine Fe-filled MWCNTs. Furthermore, both adsorption efficiency of tetracycline and enrofloxacin increased with the increased temperature. Langmuir isotherm model gave a higher correlation coefficient value than Freundlich isotherm model; thus, Langmuir model is well used to describe the adsorption for tetracycline and enrofloxacin onto pristine Fe-filled MWCNTs. The thermodynamic studies found that the adsorption of tetracycline and enrofloxacin onto pristine Fe-filled were endothermic and spontaneous nature of sorption process. In addition, the adsorption process for both tetracycline and enrofloxacin had small enthalpy change that can be inferred to physical adsorption. The adsorption equilibrium was reached within 1 hr and 3 hr for tetracycline and enrofloxacin, respectively. Their adsorption characteristics are best described by pseudo-second-order kinetic model. Thus, the synthesized Fe-filled MWCNTs are good adsorbent for removal of antibiotics from aqueous solution. Moreover, it also displayed the main advantage of easy separation.

5.2 Recommendation for Future Work

For this experiment, the application of Fe-filled MWCNTs for removal of tetracycline and enrofloxacin in aqueous solution were investigated. This experiment

proved that Fe-filled MWCNTs possessed the properties of adsorption efficiency and magnetism for easy separation. Therefore, Fe-filled MWCNTs should be used as a magnetic adsorbent to remove other kinds of antibiotics in aqueous solution. However, the synthesized Fe-filled MWCNTs should be characterized of their magnetism characteristic. In addition, effect factors of acid-treated Fe-filled MWCNTs should be studied why it cause to decrease the adsorption efficiency. Furthermore, the adsorption process for antibiotics should be designed to operate in continuous system for scale up and guideline for application in wastewater treatment system.

REFERENCES

[1] Liwei Hou, Hui Zhang and Xiaofei Xue, *Ultrasound enhanced heterogeneous activation of peroxydisulfate by magnetite catalyst for the degradation of tetracycline in water*. Separation and Purification Technology 84 (2012): 147–152.

[2] Katrin Holmström, Sara Gräslund, Ann Wahlström, Somlak Poungshompoo, Bengt-Erik Bengtsson and Nils Kautsky, *Antibiotic use in shrimp farming and implications for environmental impacts and human health*. International Journal of Food Science & Technology 38 (2003): 255 – 266.

[3] Grégorio Crini, *Recent developments in polysaccharide-basedmaterials used as adsorbents used as adsorbents in wastewater treatment*. Progress in Polymer Science 30 (2005): 38–70.

[4] Ji-Lai Gong, BinWang, Guang-Ming Zeng, Chun-Ping Yang, Cheng-Gang Niu, Qiu-Ya Niu, Wen-Jin Zho and Yi Liang, *Removal of cationic dyes from aqueous solution using magnetic multi-wall carbon nanotube nanocomposite as adsorbent*. Journal of Hazardous Materials 164 (2009): 1517–1522.

[5] Sumio Iijima, *Helical microtubules of graphitic carbon*. Nature 354 (1991): 56 – 58.

[6] Long R.Q. and Yang R.T., *Carbon nanotubes as superior sorbent for dioxin removal*. Journal of the American Chemical Society 123 (2001): 2058–2059.

[7] Kaminski M.D. and Nuñez L., *Extractant-coated magnetic particles for cobalt and nickel recovery from acidic solution*. Journal of Magnetism and Magnetic Materials 194 (1999): 31 – 36.

[8] Melissa Paradise and Tarun Goswami, *Carbon nanotubes-production and industrial applications*. Materials & Design 28 (2007): 1477-1489.

[9] Kümmerer K., *Resistance in the environment*. Journal of Antimicrobial Chemotherapy 54 (2004): 311-320.

[10] Laurence, D.R., Bennett, P.N. and Brown, M.J., *Clinical Pharmacology*, 8th ed. Churchill Livingstone, London: 1997.

[11] WHO Global Strategy for Containment of Antimicrobial Resistance, World Health Organization: 2001.

[12] Thomas J. Federici, *The non-antibiotic properties of tetracyclines: Clinical potential in ophthalmic disease*. Pharmacological Research 64 (2011): 614– 623.

[13] Allen N. Saoadin, Raul Fleischmajer, *Tetracyclines: Nonantibiotic properties and their clinical implications*. Journal of the American Academy of Dermatology 54 (2006): 258 – 265.

[14] Wan-Ru Chen and Ching-Hua Huang, *Adsorption and transformation of tetracycline antibiotics with aluminum oxide*. Chemosphere 79 (2010): 779–785.

[15] Yuan Gao, Yan Li, Liang Zhang, Hui Huang, Junjie Hu, Syed Mazhar Shah and Xingguang, *Adsorption and removal of tetracycline antibiotics from aqueous solution by graphene oxide*. Journal of Colloid and Interface Science 368 (2012): 540–546.

[16] Tillotson G.S., *Quinolones: structure-activity relationships and future predictions.* Journal of Medical Microbiology 44 (1996): 320-324.

[17] Crittenden, John C., Trussell, R. Rhodes, Hand, David W., Howe, Kerry J. and Tchobanoglous, George, *Water Treatment: Principles and Design*, 2nd ed., Wiley, New York (2005): 1260 – 1264.

[18] Roy, W.R., Krapac, I.G., Chou, S.F.J. and Griffin, R.A. *Batch-type procedures for estimating soil adsorption of chemicals*. EPA project summary (1992): 1-4.

[19] Lei Zhang, Xiaoyan Song, Xueyan Liu, Lijun Yang, Fang Pan and Junna Lv, *Studies on the removal of tetracycline by multi-walled carbon nanotubes*. Chemical Engineering Journal 178 (2011): 26– 33.

[20] Niu Liu, Ming-xia Wang, Ming-ming Liu, Fan Liu, Liping Weng, Luuk K. Koopal and Wen-feng Tan, S*orption of tetracycline on organo-montmorillonites*. Journal of Hazardous Materials 225– 226 (2012): 28–35.

[21] Hampel, S., Leonhardt, A., Selbmann, D., Biedermann, K., Elefant, D., Müller, Ch.,Gemming, T. and Büchner, B., *Growth and characterization of filled carbon nanotubes with ferromagnetic properties*. Carbon 44 (2006): 2316 – 2322.

[22] Naiqin Zhao, Chunnian He, Zhaoyang Jiang, Jiajun Li and Yongdan Li, *Fabrication and growth mechanism of carbon nanotubes by catalytic chemical vapor deposition*. Materials Letters 60 (2006): 159 – 163.

[23] Qingfeng Liu, Zhi-Gang Chen, Bilu Liu, Wencai Ren, Feng Li, Hong tao Cong and Hui-Ming Cheng, *Synthesis of different magnetic carbon nanostructures by the pyrolysis of ferrocene at different sublimation temperatures* Carbon 48 (2008): 1892 – 1902.

[24] Simone Musso, Samuele Porro, Massimo Rovere, Mauro Giorcelli and Alberto Tagliaferro, *Fluid dynamic analysis of gas flow in a thermal-CVD system designed for growth of carbon nanotubes*. Journal of Crystal Growth 310 (2008): 477 – 483.

[25] Cheng, J., Zou, X.P., Zhu, G., Wang, M.F., Su, Y., Yang, G.Q. and Lü, X.M., *Synthesis of iron-filled carbon nanotubes with a great excess of ferrocene and their magnetic properties*. Solid State Communications 149 (2009): 1619 – 1622.

[26] Tawatchai Charinpanitkul, Noriaki Sano, Pramote Puengjinda, Jiraporn Klanwan, Nattapol Akrapattangkul and Wiwut Tanthapanichakoon, *Naphthalene as an alternative carbon source for pyrolytic synthesis of*

carbon nanostructures. Journal of Analytical and Applied Pyrolysis 86 (2009) 386 – 390.

[27] Zhenyu Wang, Xiaodong Yu, Bo Pan and Baoshan Xing, *Norfloxacin sorption and its thermodynamics on surface-modified carbon nanotubes*. Environmental Science & Technology 44 (2010): 978 – 984.

[28] Carabineiro, S.A.C., Thavorn-Amornsri, T., Pereira, M.F.R. and Figueiredo, J.L., *Adsorption of ciprofloxacin on surface-modified carbon materials*. Water Research 45 (2011): 4583 – 4591.

[29] Di Zhang, Bo Pan, Min Wu, Bin Wang, Huang Zhang, Hongbo Peng, Di Wu and Ping ning, *Adsorption of sulfamethoxazole on functionalized carbon nanotubes as affected by cations and anions*. Environmental Pollution159 (2011): 2616 – 2621.

[30] Hua Chen, Hanjin Luo, Yuecen lan, Tingting Dong, Bingjie Hu and Yiping Wang, *Removal of tetracycline from aqueous solutions using polyvinylpyrrolidone (PVP-K30) modified nanoscale zero valent iron*. Journal of Hazardous Materials 192 (2011): 44– 53.

[31] Havva Merih Ötker and Işıl Akmehmet-Balcıoğlu, *Adsorption and degradation of enrofloxacin, a veterinary antibiotic on natural zeolite*. Journal of Hazardous Materials 122 (2005): 251–258.

[32] Blanchard, N.P., Hatton, R.A. and Silva S.R.P., *Tuning the work function of surface oxidized multi-wall carbon nanotubes via cation exchange*, Chemical Physics Letters 434 (2007): 92 – 95.

[33] Kevin A. Wepasnick, Billy A Smith, Kaitlin E. Schrote, Hannah K. Wilson, Stephen R. Diegelmann and Howard D. Fairbrother, *Surface and structural characterization of multi-walled carbon nanotubes following different oxidative treatments*. Carbon 49 (2011): 24 –36.

[34] Manhong Liu, Yanlian Yang, Tao Zhu and Zhongfon Liu, *Chemical modification of single-walled carbon nanotubes with peroxytrifluoroacetic acid*. Carbon 43 (2005): 1470–1478.

[35] Iosif Daniel Rosca, Fumio Wateri, Motohiro Uo and Tsukasa Akasaka, *Oxidation of multiwalled carbon nanotubes by nitric acid.* Carbon. 43 (2005): 3124–3131.

[36] Carabineiro, S.A.C., Thavorn-Amornsri, T., Pereira, M.F.R., Serp, P. and Figueiredo, J.L., *Comparison between activated carbon, and carbon xerogel and carbon nanotubes for the adsorption of the antibiotic ciprofloxacin*, Catalysis Today 186 (2012): 29-34.

[37] Jing Deng, Yisheng Shao, Naiyun Gao, Yang Deng, Chaoqun Tan, Shiqing Zhou and Xuhao Hu, *Multiwalled carbon nanotubes as adsorbents for removal of herbicide diuron from aqueous solution*. Chemical Engineering Journal 193–194 (2012): 339–347.

[38] Hui Hu, Aiping Yu, Eric Kim, Bin Zhao, Mikhail E. Itkis, Elena Bekyarova and Robert C. Haddon, *Influence of the zeta potential on the dispersability and purification of single-walled carbon nanotubes*. Journal of Physical Chemistry B 109 (2005): 11520–11524.

[39] Knapp, C.W., Cardoza, L.A., Hawes, J.N., Wellington, M.H., Larive, C.K. and Graham D. W., *Fate and Effects of Enrofloxacin in Aquatic Systems under Different Light Conditions*. Environmental Science & Technology 39 (2005): 9140-9146.

[40] Xiu-E Shen, Xiao-Quan Shan, De-Ming Dong, Xiu-Yi Hua and Gary Owens, *Kinetics and thermodynamicsof sorption of nitroaromatic compounds to as-grown and oxidized multiwalled carbon nanotubes*. Journal of Colloid and Interface Science 330 (2009): 1–8.

[41] Oliveira L.C.A., Rios R.V.R.A., Fabris J.D., Sapag K., Garg V.K. and Lago R.M., *Clay-iron oxide magnetic composites for the adsorption of contaminants in water*. Applied Clay Science 22 (2003): 169 – 177.

[42] M. A. Legodi and D. de Waal, *The preparation of magnetite, goethite, hematite and maghemite of pigment quality from mill scale iron waste*. Dyes and Pigments 74 (2007): 161–168.

[43] Nattapol Akrapattangkul, *Removal of dye pollutants using multi-walled carbon nanotubes with magnetic characteristics*, Master's Thesis, Department of Chemical Engineering, Faculty of Engineering, Chulalongkorn University (2010): 28 – 33.

APPENDICES

APPENDIX A
IRON – CARBON PHASE DIAGRAM

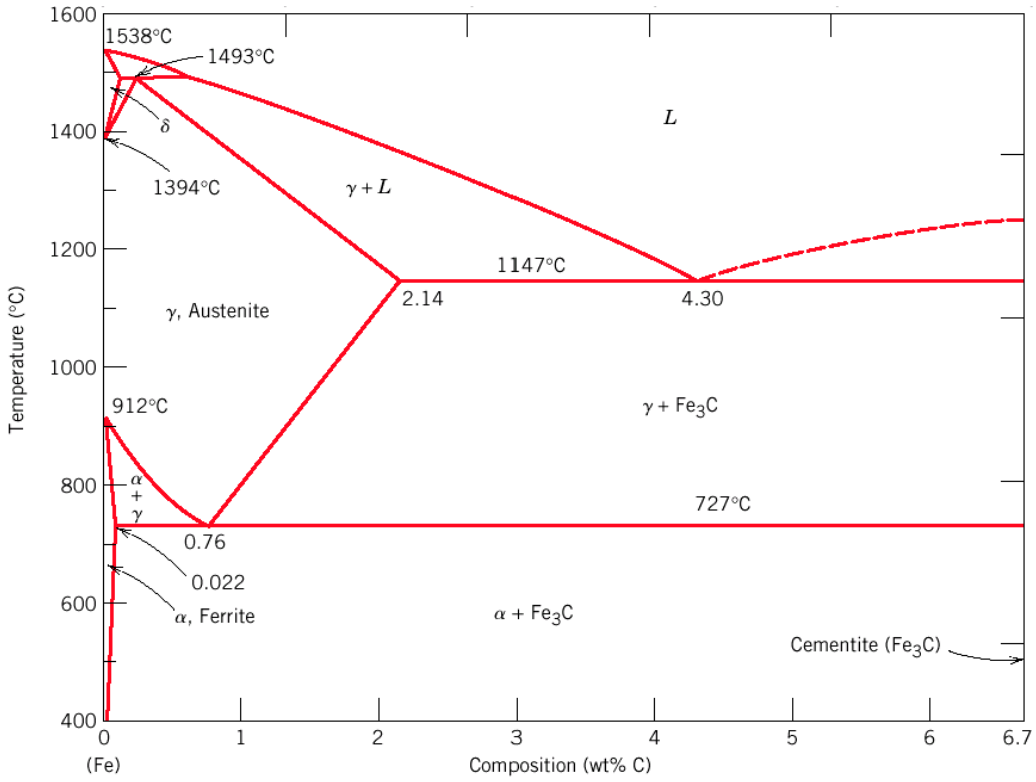

Figure A.1 The Fe–C Phase Diagram
(http://web.utk.edu/~prack/MSE%20300/FeC.pdf)

The Fe–C phase diagram shows which phases are to be expected at metastable equilibrium for different combination of carbon content and temperature. At low-carbon end of the Fe-C phase diagram, ferrite (α-Fe) which can dissolve 0.022 wt% of C at 738^{o}C that is stable form of iron at room temperature. When the temperature increased to 912^{o}C, it can transform to FCC austenite (γ-Fe). Austenite can dissolve 2.14 wt% of C at 1154^{o}C that is not stable below the eutectic temperature (727^{o}C) unless cooled rapidly. Moreover, when the temperature increased to 1395^{o}C austenite can transform to BBC delta-ferrite (δ-Fe). At the carbon-rich side of the Fe-C phase diagram it is iron carbide or cementite (Fe_3C). This intermetallic compound is

metastable that it remains as a compound indefinitely at room temperature, but decomposes into ferrite (α-Fe) and C (graphite) at 650 – 700^{o}C. The magnetic property of ferrite (α-Fe) is below 768^{o}C while austenite (γ-Fe) is non-magnetic.

APPENDIX B
STANDARD CURVE OF TETRACYCLINE AND ENROFLOXACIN

Table B.1 Concentrations and absorbance of tetracycline (TTC) at pH = 7±0.5 (λ_{max} = 359 nm)

Concentrations (mg/L)	Absorbance
10	0.357
20	0.681
30	1.025
40	1.371
50	1.695
60	2.051
70	2.339
80	2.627
90	2.992
100	3.248

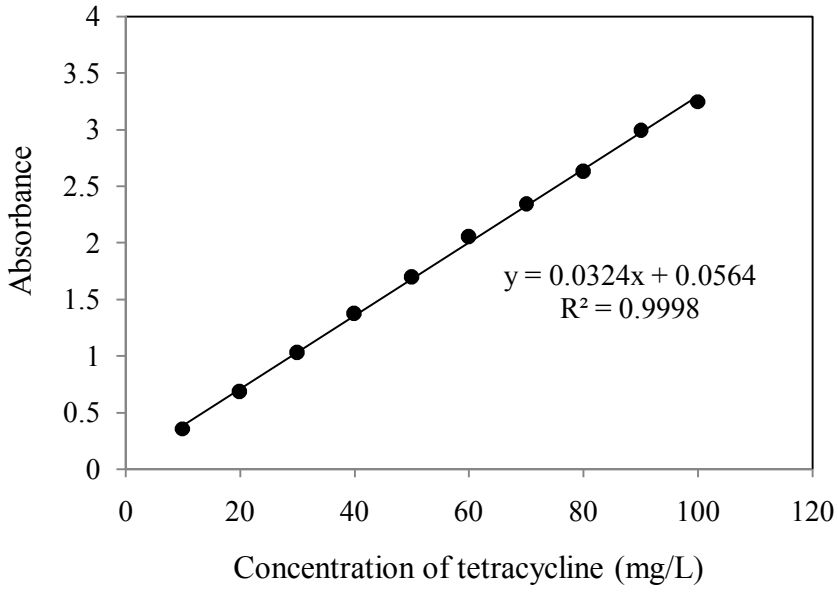

Figure B.1 Standard Curve of tetracycline (TTC) at pH = 7±0.5 (λ_{max} = 359 nm)

Table B.2 Concentrations and absorbance of enrofloxacin (ENR) at pH = 7±0.5 (λ_{max} = 323 nm)

Concentrations (mg/L)	Absorbance
10	0.307
20	0.63
30	0.939
40	1.248
50	1.558
60	1.854
70	2.158
80	2.41

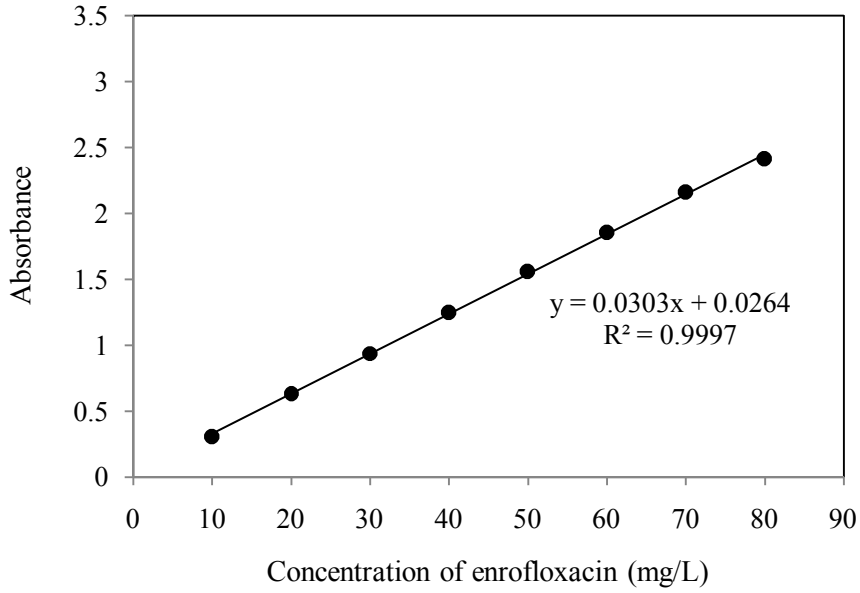

Figure B.2 Standard Curve of enrofloxacin (ENR) at pH = 7±0.5 (λ_{max} = 323 nm)

APPENDIX C
BATCH ADSORPTION EXPERIMENTAL

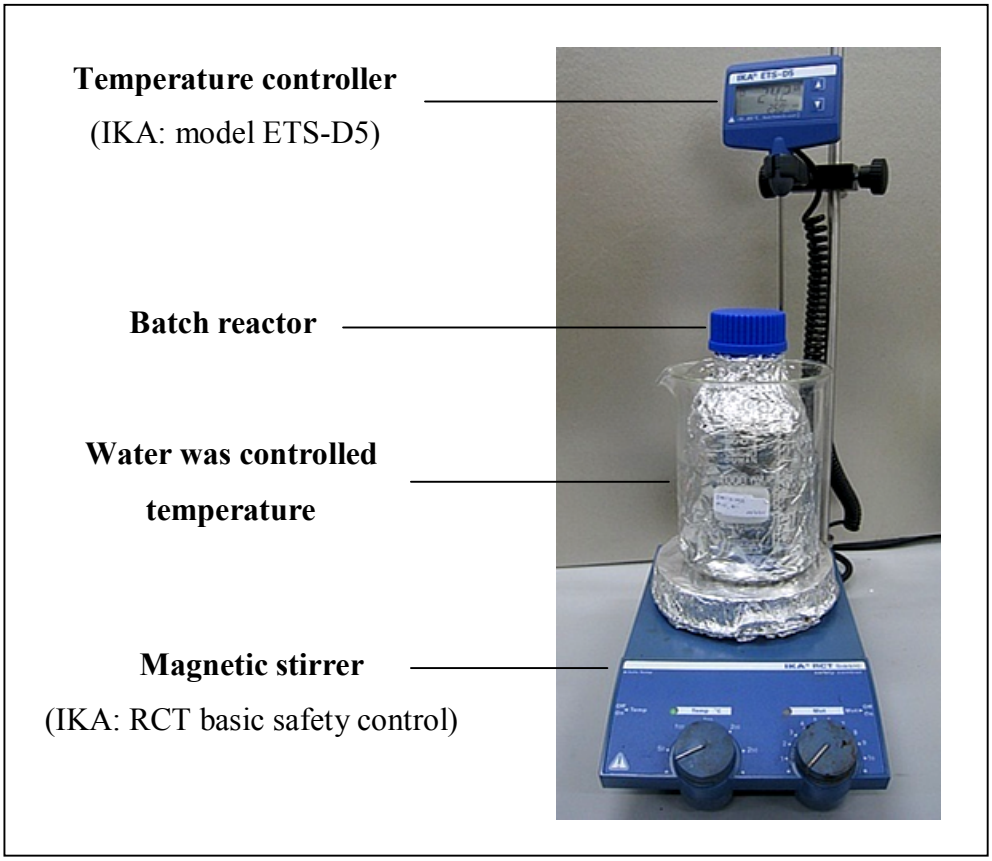

Figure C.1 The photograph of batch adsorption system

APPENDIX D

BATCH EQUILIBRIUM ADSORPTION ISOTHERMS

Table D.1 Langmuir adsorption isotherms of tetracycline at 25°C and pH = 7±0.5

Initial concentration (C_0) (mg/L)	Equilibrium concentration (C_e) (mg/L)	Equilibrium adsorption capacity (Q_e) (mg/g)	C_e/Q_e (g/L)
10.218	0.104	31.606	0.003
25.563	1.077	76.519	0.014
40.313	4.879	110.731	0.044
55.219	14.116	128.447	0.110
70.406	26.351	137.672	0.191
85.281	38.042	147.622	0.258
100.531	49.856	158.359	0.315

Table D.2 Langmuir adsorption isotherms of tetracycline at 40°C and pH = 7±0.5

Initial concentration (C_0) (mg/L)	Equilibrium concentration (C_e) (mg/L)	Equilibrium adsorption capacity (Q_e) (mg/g)	C_e/Q_e (g/L)
10.218	0.067	31.722	0.002
25.563	0.879	77.138	0.011
40.313	3.272	115.753	0.028
55.219	9.213	143.769	0.064
70.406	18.675	161.659	0.116
85.281	31.164	169.116	0.184
100.531	42.781	180.469	0.237

Table D.3 Langmuir adsorption isotherms of tetracycline at 55°C and pH = 7±0.5

Initial concentration (C_0) (mg/L)	Equilibrium concentration (C_e) (mg/L)	Equilibrium adsorption capacity (Q_e) (mg/g)	C_e/Q_e (g/L)
10.218	0.031	31.834	0.001
25.563	0.475	78.400	0.006
40.313	1.073	122.625	0.009
55.219	4.517	158.445	0.029
70.406	10.998	185.650	0.059
85.281	22.714	195.522	0.116
100.531	35.882	202.028	0.178

Table D.4 Langmuir adsorption isotherms of enrofloxacin at 25°C and pH = 7±0.5

Initial concentration (C_0) (mg/L)	Equilibrium concentration (C_e) (mg/L)	Equilibrium adsorption capacity (Q_e) (mg/g)	C_e/Q_e (g/L)
10.115	2.612	23.447	0.111
30.348	14.737	48.784	0.302
50.152	33.961	50.599	0.671
70.267	52.468	55.622	0.943

Table D.5 Langmuir adsorption isotherms of enrofloxacin at 40°C and pH = 7±0.5

Initial concentration (C_0) (mg/L)	Equilibrium concentration (C_e) (mg/L)	Equilibrium adsorption capacity (Q_e) (mg/g)	C_e/Q_e (g/L)
10.115	2.242	24.603	0.091
30.348	12.646	55.319	0.229
50.152	29.679	63.978	0.464
70.267	49.327	65.438	0.754

Table D.6 Langmuir adsorption isotherms of enrofloxacin at 55°C and pH = 7±0.5

Initial concentration (C_0) (mg/L)	Equilibrium concentration (C_e) (mg/L)	Equilibrium adsorption capacity (Q_e) (mg/g)	C_e/Q_e (g/L)
10.115	1.989	25.394	0.078
30.348	10.537	61.909	0.170
50.152	26.832	72.875	0.368
70.267	46.676	73.722	0.633

Table D.7 Freundlich adsorption isotherms of tetracycline at 25°C and pH = 7±0.5

Initial concentration (C_0) (mg/L)	Equilibrium concentration (C_e) (mg/L)	Equilibrium adsorption capacity (Q_e) (mg/g)	log C_e	log Q_e
10.218	0.104	31.606	-0.983	1.450
25.563	1.077	76.519	0.032	1.884
40.313	4.879	110.731	0.688	2.044
55.219	14.116	128.447	1.150	2.109
70.406	26.351	137.672	1.421	2.139
85.281	38.042	147.622	1.580	2.169
100.531	49.856	158.359	1.698	2.120

Table D.8 Freundlich adsorption isotherms of tetracycline at 40°C and pH = 7±0.5

Initial concentration (C_0) (mg/L)	Equilibrium concentration (C_e) (mg/L)	Equilibrium adsorption capacity (Q_e) (mg/g)	log C_e	log Q_e
10.218	0.067	31.722	-1.174	1.501
25.563	0.879	77.138	-0.056	1.887
40.313	3.272	115.753	0.515	2.064
55.219	9.213	143.769	0.964	2.158
70.406	18.675	161.659	1.271	2.209
85.281	31.164	169.116	1.494	2.228
100.531	42.781	180.469	1.631	2.256

Table D.9 Freundlich adsorption isotherms of tetracycline at 55°C and pH = 7±0.5

Initial concentration (C_0) (mg/L)	Equilibrium concentration (C_e) (mg/L)	Equilibrium adsorption capacity (Q_e) (mg/g)	log C_e	log Q_e
10.218	0.031	31.834	-1.509	1.503
25.563	0.475	78.400	-0.323	1.894
40.313	1.073	122.625	0.031	2.089
55.219	4.517	158.445	0.655	2.200
70.406	10.998	185.650	1.041	2.269
85.281	22.714	195.522	1.356	2.291
100.531	35.882	202.028	1.5552	2.305

Table D.10 Freundlich adsorption isotherms of enrofloxacin at 25°C and pH = 7±0.5

Initial concentration (C_0) (mg/L)	Equilibrium concentration (C_e) (mg/L)	Equilibrium adsorption capacity (Q_e) (mg/g)	log C_e	log Q_e
10.115	2.612	23.447	0.417	1.370
30.348	14.737	48.784	1.168	1.688
50.152	33.961	50.599	1.531	1.704
70.267	52.468	55.622	1.720	1.745

Table D.11 Freundlich adsorption isotherms of enrofloxacin at 40°C and pH = 7±0.5

Initial concentration (C_0) (mg/L)	Equilibrium concentration (C_e) (mg/L)	Equilibrium adsorption capacity (Q_e) (mg/g)	log C_e	log Q_e
10.115	2.242	24.603	0.351	1.391
30.348	12.646	55.319	1.102	1.743
50.152	29.679	63.978	1.472	1.806
70.267	49.327	65.438	1.693	1.816

Table D.12 Freundlich adsorption isotherms of enrofloxacin at 55°C and pH = 7±0.5

Initial concentration (C_0) (mg/L)	Equilibrium concentration (C_e) (mg/L)	Equilibrium adsorption capacity (Q_e) (mg/g)	log C_e	log Q_e
10.115	1.989	25.394	0.299	1.405
30.348	10.537	61.909	1.023	1.792
50.152	26.832	72.875	1.427	1.863
70.267	46.676	73.722	1.6691	1.868

APPENDIX E
LIST OF PUBLICATIONS

Kanokwan Sowichai, Sitthisuntorn Supothina, On-uma Nimittrakoolchai, Takafumi Seto, Yoshio Otani and Tawatchai Charinpanitkul, "Preparation of Magnetic Multi-Walled Carbon Nanotubes" Oral Presentation on Chemistry for Global Warming, Green Energy & Environment. Proceeding of the 6th Pure and Applied Chemistry International Conference 2012 (PACCON 2012), Changmai, Thailand, January 11 – 13, 2012.

Kanokwan Sowichai, Sitthisuntorn Supothina, On-uma Nimittrakoolchai, Takafumi Seto, Yoshio Otani and Tawatchai Charinpanitkul, "Facile method to prepare magnetic multi-walled carbon nanotubes by in situ co-precipitation route". Journal of Industrial and Engineering Chemistry 18 (2012): 1568–1571.

VITA

Miss Kanokwan Sowichai was born in September 14, 1987, in Chaiyaphoom, Thailand. She completed her high-school education at Nongbuapittayakarn School, in Nongbualamphoo, in 2006. She entered to Department of Chemical Engineering, Faculty of Engineering, Ubon Ratchathani University. After graduation the degree of Bachelor, in 2010, she decided continuously to study in Master degree in Center of Excellence in Particle Technology at Department of Chemical Engineering, Faculty of Engineering, Chulalongkorn University. She obtained the this degree with the thesis entitled “Application of Fe-filled multi-walled carbon nanotubes for removal of antibiotics from aqueous solution”